KINETICS OF ROULEAU FORMATION

I. A Mass Action Approach with Geometric Features

RICHARD W. SAMSEL
Division of Biology and Medicine, Brown University, Providence, Rhode Island 02912

ALAN S. PERELSON
Theoretical Division, University of California, Los Alamos National Laboratory, Los Alamos, New Mexico 87545 and Division of Biology and Medicine, and Lefschetz Center for Dynamical Systems, Brown University, Providence, Rhode Island 02912

ABSTRACT In the presence of certain macromolecules, such as fibrinogen, immunoglobulin, dextran, and polylysine, erythrocytes tend to aggregate and form cylindrical clusters called "rouleaux" in which cells resemble coins in a stack. The aggregates may remain cylindrical or they may branch, forming tree, and networklike structures. Using the law of mass action and notions from polymer chemistry, we derive expressions describing the kinetics of the early phase of aggregation. Our models generalize work initiated by Ponder in 1927 who used the Smoluchowski equation to predict the concentration of rouleaux of different sizes. There are two novel features to our generalization. First, we allow erythrocytes that collide near the end of a stack of cells to move to the end of the cylinder and elongate it. Second, we incorporate geometric information into our models and describe the kinetics of branched rouleau formation. From our models we can predict the concentration of rouleaux with n cells and b branches, the mean number of cells per rouleau, the mean number of branches per rouleau, and the average length of a branch. Comparisons are made with the available experimental data.

I. INTRODUCTION

Erythrocytes that are normally monodisperse tend to aggregate in the presence of certain macromolecules. The aggregates that form may be completely irregular, with the erythrocytes in the cluster having arbitrary orientation with respect to one another, as seen in the hemagglutination reaction used to type blood (cf. Thygesen, 1942), or the aggregates may be long cylindrical objects called "rouleaux," in which cells adhere face to face and resemble coins in a stack. Large rouleaux are commonly branched. Examples of both linear and branched rouleaux are shown in Fig. 1. Because rouleaux form in human blood they have been the object of intensive study for over 200 years (see Fähraeus, 1921, and Thygesen, 1942, for historical reviews). The adhesion responsible for the ordered aggregation seen in rouleau formation is thought to be mediated by intercellular bridges formed by macromolecules simultaneously adsorbed on opposing faces of the adherent cells (Jan, 1979*a*; Chien, 1980, 1981). The tendency to form rouleaux and the shape of the rouleaux formed reflect the membrane mechanics of the red cell, and depend upon the strength of binding between the cells (Chien et al., 1978). At extremely high adhesive energies disordered aggregates form rather than rouleaux (Chien, 1981). As might be expected, the degree of erythrocyte aggregation is a function of the type and concentration of the macromolecules used (Merrill et al., 1969), of the shear rate in the suspending fluid (Usami et al., 1975), of temperature (Dintenfass and Forbes, 1973), of ionic strength (Jan and Chien, 1973*b*), and of the charge on the red cells (Jan and Chien, 1973*a*). Although many of the considerations we raise in this paper apply to the disordered aggregates formed by agglutination reactions, we shall restrict our attention to rouleaux.

While rouleau formation is interesting as a model system for the study of cellular adhesion and aggregation, it is also physiologically significant in microcirculatory hemodynamics. Aggregation in vivo usually involves fibrinogen (Chien et al., 1967) or serum globulins (Dintenfass and Somer, 1975). Rouleaux are sensitive to the flow regime of the fluid in which they are suspended (Usami et al., 1975). At high shear rates, rouleaux are rapidly broken up, and red cells are monodisperse. In the absence of shear, red cells collide only rarely, so aggregation proceeds very slowly. Low shear rates induce red cell aggregation, presumably by increasing the collision frequency without inducing sufficient mechanical forces to disaggregate the cells. Largely as a result of rouleau formation, the viscosity of blood increases as the rate of shear decreases (Whitmore, 1968; Chien et al., 1973). Blood shows thixotropy (Huang et al., 1975) and, at low shear rates, viscoelasticity

Reprint requests should be sent to Dr. Perelson

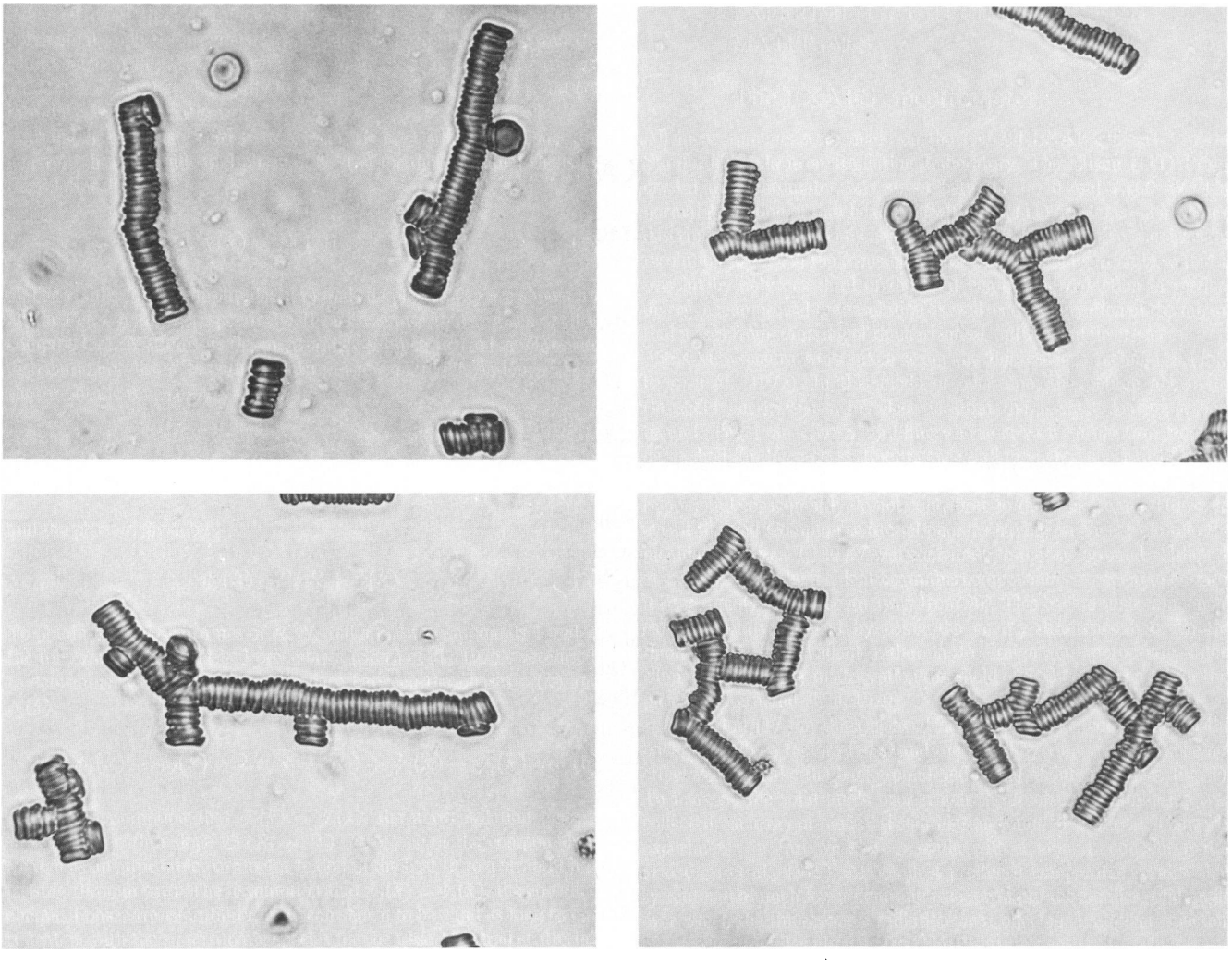

FIGURE 1 Typical rouleaux. Fresh blood from a healthy individual, anticoagulated with EDTA, was centrifuged and resuspended in its own plasma at a hematocrit of 1%. A drop of the resulting suspension was placed on a microscope slide, covered with a glass cover slip, and photographed with phase contrast optics.

(Chien et al., 1975). The "anomalous viscosity" of blood is apt to be most significant in the microcirculation, and is generally attributed to the formation of rouleaux and to the ability of red cells to deform (Fung, 1981).

Erythrocyte aggregation is used clinically as an index of the concentration of macromolecules in the blood plasma. The erythrocyte sedimentation rate, a measure of red cell aggregation, is elevated in several diseases including multiple myeloma, many infections, macroglobulinemias, some malignancies, and diabetes mellitus (cf. Reich, 1978). Intravascular aggregation can lead to a slowing of microvascular blood flow, resulting in localized hypoxia and acidosis (Dintenfass, 1976). In patients with diabetes mellitus, increased aggregation may play a role in the pathogenesis of vascular derangements and diabetic retinopathy (Dintenfass, 1977).

The adhesive aspects of rouleau formation have been examined in model systems using dextrans (Brooks and Seaman, 1973) and polylysines (Katchalsky et al., 1959) with various molecular weights. The macromolecular bridging hypothesis reviewed by Chien (1980, 1981), is supported by the electron microscopic observation that the distance between adherent cell surfaces increases directly with the length of the bridging macromolecule (Katchalsky et al., 1959; Chien and Jan, 1973). Dextran-induced aggregation is inhibited by urea, and therefore is probably due to hydrogen bonding between the dextran and the cell surface (Jan, 1979*b*). Fluid mechanical techniques have been used to show that the adherence of red cells in a rouleau is reversible: two partially separated red cells move back together when an applied shear stress is removed (Chien et al., 1977); high shear rates break up even the largest of rouleaux (Usami et al., 1975).

A theoretical picture of the adhesion process in rouleau formation is emerging. Negatively charged red cells repel one another electrostatically, but may be bridged by macromolecules. If the energy of cell adhesion due to the adsorption of macromolecules is greater than the electro-

static repulsive energy, adhesion is favored (Chien, 1975). There may be some contribution to the net energy per unit area due to short range van der Waals forces, but their influence does not seem to be dominant (Jan, 1979*b*). After initial contact between the cells (due to random or shear-induced collisions), the contact area increases until the adhesive force is balanced by the force of membrane elasticity (Skalak et al., 1977).

The clinical consequences of rouleau formation are correlated with the effects of the aggregate on the microcirculation. These in turn are directly related to the size and shape of the rouleau. Our goal in this paper is to develop a mathematical model for the kinetics of rouleau formation that will allow us to predict the number of cells in a rouleau and the degree of branching in its structure. Our work is a generalization of a model proposed by Ponder (1927). Ponder treated rouleau formation as an irreversible linear polycondensation reaction, adapting the solution of the Smoluchowski equation of coagulation kinetics to the problem of rouleau formation. However, Ponder dismissed the problem of branching of rouleaux under the assumption that branches are inherently unstable structures which do not effect the aggregates ultimately seen. Although this may be true to some extent, we shall see that branching can have important effects on the kinetics of rouleau formation. Branched rouleaux, even if constantly being formed and degraded, would be expected to play a predominant role in microcirculatory dynamics. Hydrodynamic aspects of rouleau formation will not be dealt with here, although we note that Adler (1979) has attempted to predict the size of a rouleau in a sedimentation field on this basis. The equilibrium distribution of rouleau sizes has been studied by Perelson and Wiegel (1982). Here we restrict our attention to the early phases of rouleau formation in which reactions can be thought of as being irreversible.

In modeling rouleau formation as a polymerization reaction we shall implicitly make various assumptions about the physical processes leading to collisions among red cells and red cell aggregates. To each reaction we assign a rate constant, k. Although we shall treat these rate constants as "constants," their values will depend on the physical variables that characterize an experiment, e.g., the temperature and viscosity of suspending medium, the concentration and type of bridging macromolecule, and the detailed fluid flows set up in the experimental apparatus. In polymerization reactions molecules are usually brought together by Brownian motion. Stirring and other external fluid motions induced in the medium have a neglible effect compared with diffusion in bringing two particles together when their radius is <0.05 μm (Purcell, 1978). For particles as large as red cells the opposite is true. Brownian motion can be ignored, and sedimentation and fluid motion become the predominant forces influencing particle collisions. Although these forces are not isotropic, we shall assume that one can find an appropriate average rate constant which is the same at all positions within the volume. Furthermore, we initially assume k to be independent of particle size, although in section III we introduce rate constants that are proportional to rouleau surface area. At later stages in modeling one can develop more refined methods of choosing k. For example, theories of aggregation in shear fields are discussed by Bell (1981), Richardson (1973), Swift and Friedlander (1964), and Levich (1962). Jones and Perry (1979) describe a theory for the aggregation of cells in turbulent flow fields based upon work of Saffman and Turner (1956). The geometry and frequency of two-body collisions has been studied in dilute suspensions of spheres and disks undergoing Couette and Poiseuille flow in both Newtonian (Goldsmith and Mason, 1967) and non-Newtonian media (Gauthier et al., 1971*a*, *b*). Utilizing these theories alone will prove incomplete in modeling of rouleau formation. For though fluid flow affects the rate of aggregation, the presence of aggregates in turn influences the fluid flow. For example, at low rates of shear, blood flow obeys the Casson equation (Fung, 1981; Cokelet et al., 1963). This non-Newtonian behavior is felt to reflect red cell aggregation, among other processes. There is to our knowledge no complete theory of aggregation and fluid flow that can predict collision rates between growing aggregates in a changing fluid environment. As theoretical results become available, more refined assumptions regarding the values of k can be made. In this paper our major focus shall be on formulating the correct kinetic equations to describe the aggregation process, assuming appropriate rate constants can be found from some other theory. Here we shall assume that k is a constant whose value is to be determined for each particular experimental situation.

In section II we describe Ponder's work and our generalizations for predicting the number of cells in a rouleau. In section III we consider the effects of geometry and develop a model for the formation of branched rouleaux. A discussion of our results follows in section IV.

II. NUMBER OF CELLS IN A ROULEAU

Theories of Polymerization

The basic ideas developed in polymer chemistry for describing the formation of large polymeric molecules can be applied to many types of aggregation processes. For example, Smoluchowski's theory of the coalescence of liquid droplets (Smoluchowski, 1916, 1917) is formally equivalent to a special case of the theory of condensation polymerization (cf. Ziff, 1980). Here we shall illustrate how to describe the kinetics of rouleau formation using the theories of addition and condensation polymerization. Ponder (1927) initiated this approach by applying the Smoluchowski equation to irreversible rouleau formation. Chang and Robertson (1976) used this method for studying platelet aggregation and more recently Ryan et

al. (1980) used it to analyze the dextran-induced aggregation of bacteria.

A rouleau containing n red cells will be referred to as an n-mer. There are two classes of reactions that we shall consider: addition reactions

$$n\text{-mer} + 1\text{-mer} \rightarrow (n+1)\text{-mer},$$

and condensation reactions

$$n\text{-mer} + i\text{-mer} \rightarrow (n+i)\text{-mer}.$$

Addition polymerization reactions involve the sequential addition of monomer to growing polymer chains, whereas condensation reactions allow polymer chains of all sizes to interact.

In rouleau formation both mechanisms may be operative, single cells can add to growing rouleaux, and two rouleaux may collide and form a larger rouleau. Because single cells are more mobile than rouleaux, we first examine the consequences of a pure addition model and later examine more realistic models that incorporate both addition and condensation. Also, to simplify our development, we treat all reactions as if they were irreversible. Thus our models will only be valid for times that are short compared with the time needed to establish equilibrium. In a later paper we shall incorporate the kinetics of dissociative processes, and study the long time behavior of red cell aggregation phenomena.

Application of Addition Polymerization to Rouleau Formation

If single red cells add to the ends of growing rouleaux, addition polymerization may be considered as a model for rouleau formation. Rouleaux are initiated when two erythrocytes collide and adhere. Since individual red cells may have different properties than rouleaux with regard to their membrane mechanics and collision rate, we allow two different rate constants: k_e, the rate constant for the reaction between two erythrocytes, and k_a, the rate constant for addition of an erythrocyte to a rouleau. We denote the concentration of free erythrocytes at time t by $E(t)$, and the concentration of rouleaux with n cells by $R(n, t)$. At $t = 0$, we assume the erythrocyte concentration is E_0 and no rouleaux are present. Let

$$R(t) \equiv \sum_{n=2}^{\infty} R(n, t) \tag{1}$$

be the total concentration of rouleaux at time t, irrespective of size.

Elongation of existing rouleaux conserves the number of rouleaux, so $R(t)$ is affected only by the production or destruction of new two-cell rouleaux. If erythrocytes collide at random then the square of their concentration is proportional to their collision frequency. Therefore, neglecting dissociation, we can write

$$dR/dt = \tfrac{1}{2} k_e E^2, \tag{2}$$

with the initial condition

$$R(0) = 0. \tag{3}$$

We have included a statistical factor of ½ in the erythrocyte-erythrocyte reaction rate since identical particles are interacting. It arises because the relative rate of collisions between particles labeled A, B, C, etc. is proportional to A^2, 2AB, B^2, 2AC, etc.; i.e., identical particles collide with half the frequency of distinguishable particles (Tanford, 1961, p. 589). This factor can be included in the rate constant k_e, but for reasons of consistency which will become apparent later we have decided not to make this simplification.

Two erythrocytes are lost by each occurrence of the initiation reaction, and one disappears by each collision with an existent rouleau. Hence,

$$dE/dt = -k_e E^2 - k_a E R, \tag{4}$$

with initial condition

$$E(0) = E_0. \tag{5}$$

We can also write an equation for the rate of change of any individual species of rouleau

$$dR(2)/dt = \tfrac{1}{2} k_e E^2 - k_a E R(2), \tag{6}$$

and

$$dR(n)/dt = k_a E [R(n-1) - R(n)], \quad n = 3, 4.... \tag{7}$$

In the addition mechanism, n-cell rouleaux are formed by the collision of an erythrocyte with an $(n-1)$-cell rouleau, and disappear when an erythrocyte adds to an n-cell rouleau to form an $(n+1)$-cell rouleau. In Eqs. 6 and 7, for simplicity, we have abbreviated $R(n, t)$ to $R(n)$. To denote the initial condition we include the time dependence. Thus, the initial conditions for Eqs. 6 and 7 are

$$R(n, 0) = 0, \qquad n = 2, 3.... \tag{8}$$

In Fig. 2 we show the results of numerically integrating the equations for this addition polymerization model. Our results are plotted in terms of the following nondimensional variables:

$$E' = E/E_0, \quad R' \; R/E_0, \quad R'(n) = R(n)/E_0, t' = tk_aE_0, \tag{9a}$$

and a nondimensional rate constant

$$k_e' = k_e/k_a. \tag{9b}$$

From Fig. 2 we can see the following general trends: free erythrocytes, E, decrease monotonically, whereas total

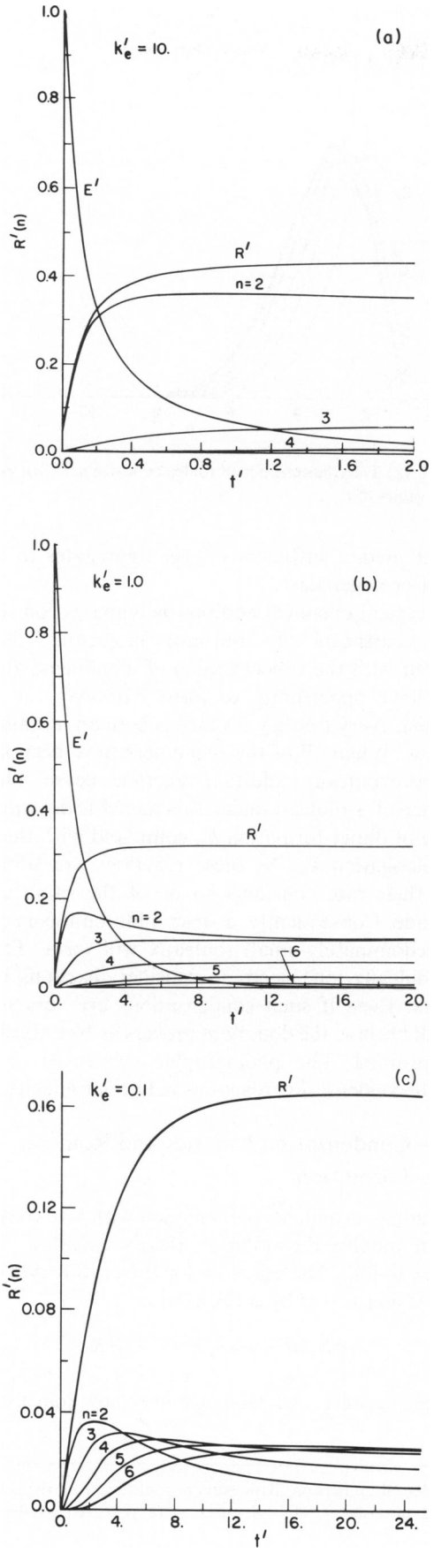

rouleaux constantly increase. Initially, the predominant rouleaux are dimers. Although we expect k'_e to be of order 1, we have explored a reasonably wide parameter range in our simulations. When $k'_e \gg 1$ (Fig. 2 *a*) erythrocyte-erythrocyte collisions occur more frequently than erythrocyte-rouleau collisions. Thus dimers remain the most prevalent species. When $k'_e = 1$ (Fig. 2 *b*) dimer formation and chain elongation occur with equal rates and aggregates with three, four, and five cells occur in appreciable numbers. Lastly, if $k'_e \ll 1$ (Fig. 2 *c*) chain elongation occurs more frequently than dimer formation. Hence, once a two-cell rouleau is formed it quickly becomes a trimer. Similarly, three-cell rouleaux quickly convert to four-cell rouleaux and so on. Thus as Fig. 2 *c* shows, the predominant species changes sequentially from two-cell to three-cell to larger rouleaux.

Other ways to display this data are to examine for fixed times the number distribution of rouleau $R'(n)$, or the number of red cells in rouleaux, $nR'(n)$. In Fig. 3*a* we plot for $k'_e = 1$, $R'(n)$ vs. n for $t' = 1, 2, 3, 5, 8$, and 10. At large values of t' the curves superimpose indicating that a steady-state distribution is being approached. A plot of $R'(n)$ vs. n will be called the "rouleau number distribution, inasmuch as it indicates the number or, more precisely, the concentration of rouleau of size n. In Fig. 3 *b*, we plot for $k'_e = 1$, $nR'(n)$ vs. n for various t'. This plot, which we call the "rouleau weight distribution" or the "red cell distribution," indicates how the red cells are distributed among the various rouleaux. Here we see that at $t' = 10$ the majority of red cells are in three-cell rouleaux, even though two-cell rouleaux are the most prevalent species (Fig. 3 *a*).

For $k'_e = 2$ we can analytically determine the concentration of erythrocytes and the total rouleau concentration in the limit as $t \to \infty$ (see Appendix I). For other values of k'_e these limiting concentrations can be found numerically. Table I shows the results of numerically integrating the nondimensional form of Eqs. 2 and 4 (Eqs. A1.1 and A1.2) to time $t' = 20$, for different values of k'_e.

The parameter U, listed in Table I, is the mean size of the units in suspension. In terms of dimensional variables

$$U = E_0/(E + R) . \tag{10}$$

The numerator represents the total number of erythrocytes, and the denominator represents the total number of units (red cells and rouleaux) each expressed per unit volume. The ratio is the mean "size" of, or number of cells in, a unit. This quantity becomes negligibly different from the mean size of a rouleau when the aggregation process is

FIGURE 2 The kinetics of rouleau formation with a pure addition mechanism. R' is the total concentration of rouleaux, $R'(n)$, $n = 2, 3, \ldots$ is the concentration of rouleaux with n cells and E' is the free erythrocyte concentration. All variables are nondimensional. (*a*) $k'_e = 10.$, (*b*) $k'_e = 1.$, (*c*) $k'_e = 0.1$.

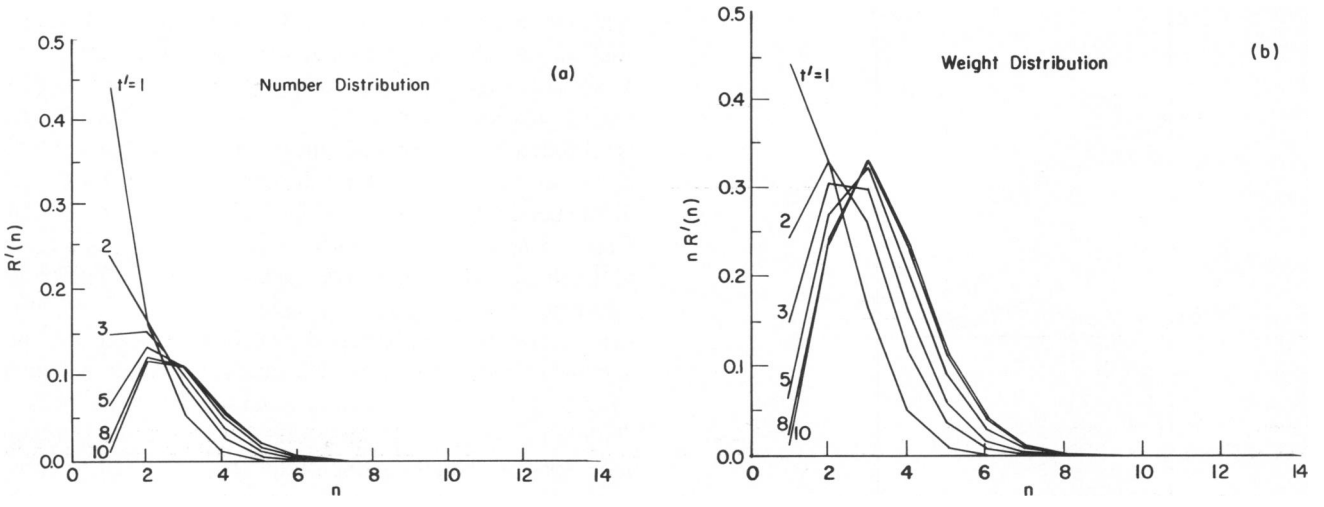

FIGURE 3 The distribution of rouleaux for a pure addition mechanism with $k'_e = 1$. (*a*) The concentration of rouleaux of size n, $R'(n)$, vs. n, (*b*) the concentration of erythrocytes in rouleaux of size n, $nR'(n)$, vs. n for various values of t'.

TABLE I
THE NONDIMENSIONAL CONCENTRATIONS OF ROULEAUX, R', FREE ERYTHROCYTES, E', AND THE MEAN SIZE OF UNITS IN SUSPENSION, $U = 1/(E' + R')$, AT TIME $t' = 20$ FOR VARIOUS VALUES OF k'_e

k'_e	R'	E'	U
0.1	0.1641	0.0334	5.065
0.2	0.2085	0.0104	4.569
0.4	0.2571	0.0028	3.848
1.0	0.3224	4×10^{-4}	3.098
2.0	0.3679	1×10^{-4}	2.717
4.0	0.4066	3×10^{-5}	2.459
10.0	0.4452	1×10^{-5}	2.246

nearly complete because E approaches zero. Note that for $k'_e = 2$, the computed value at $t' = 20$ of U (2.717) is already quite close to its asymptotic value (2.718), found in Appendix I.

From the data in Table I, we see that the asymptotic mean rouleau size is approximately three cells for $k'_e = 1$. This is in agreement with the maximal value of the mean unit size (also called the microscopic aggregation index, or MAI, in the literature) found experimentally by Chien (1973) at low cell densities and using dextran as the bridging macromolecule. By contrast when fibrinogen is used, mean unit sizes of up to eight cells are found (Jan and Chien, 1973*c*). Thus, a comparison to published data on the average size of a unit shows that the addition theory predicts a realistic mean aggregate size for dextran systems when E_0 is small (i.e., at low cell densities). However, the addition model for reasonable values of k'_e does not predict sufficiently large aggregates to account for the fibrinogen data.

In a typical chemical addition polymerization reaction, the concentration of "initiator molecules" is small compared with the concentration of monomers, and large chains have opportunity to form. However, in rouleau formation, every free erythrocyte is both an initiator and a monomer. When all of the monomers have been incorporated into rouleaux, addition reactions cease. Thus, the mean size of a rouleau under this model is determined by the rate of dimer formation k_e, compared with the rate of chain elongation k_a. As these reactions are similar, we expect their rate constants to be of the same order of magnitude. Consequently, a strict addition theory predicts that predominately small rouleaux will form. To obtain large rouleaux, one needs to consider reactions between rouleaux. Even if such condensations are very unlikely, they will become the dominant process as free erythrocytes are consumed. The photographic sequences in Fig. 4 illustrate condensation reactions between rouleaux.

Condensation Kinetics and Rouleau Formation

By including a condensation reaction with rate constant k_c, one can modify the addition theory to allow any two rouleaux to join. The equation for the erythrocyte concentration is unaffected by condensation,

$$dE/dt = -k_e E^2 - k_a ER . \qquad (11)$$

However, because two rouleaux may now join to form a

FIGURE 4 Condensation of rouleaux. Two sequences of photomicrographs, taken under oil immersion, show pairs of rouleaux from the time of first adhesion through the process of alignment. Each sequence spans a time period of order 1 min. Samples were prepared as described in Fig. 1.

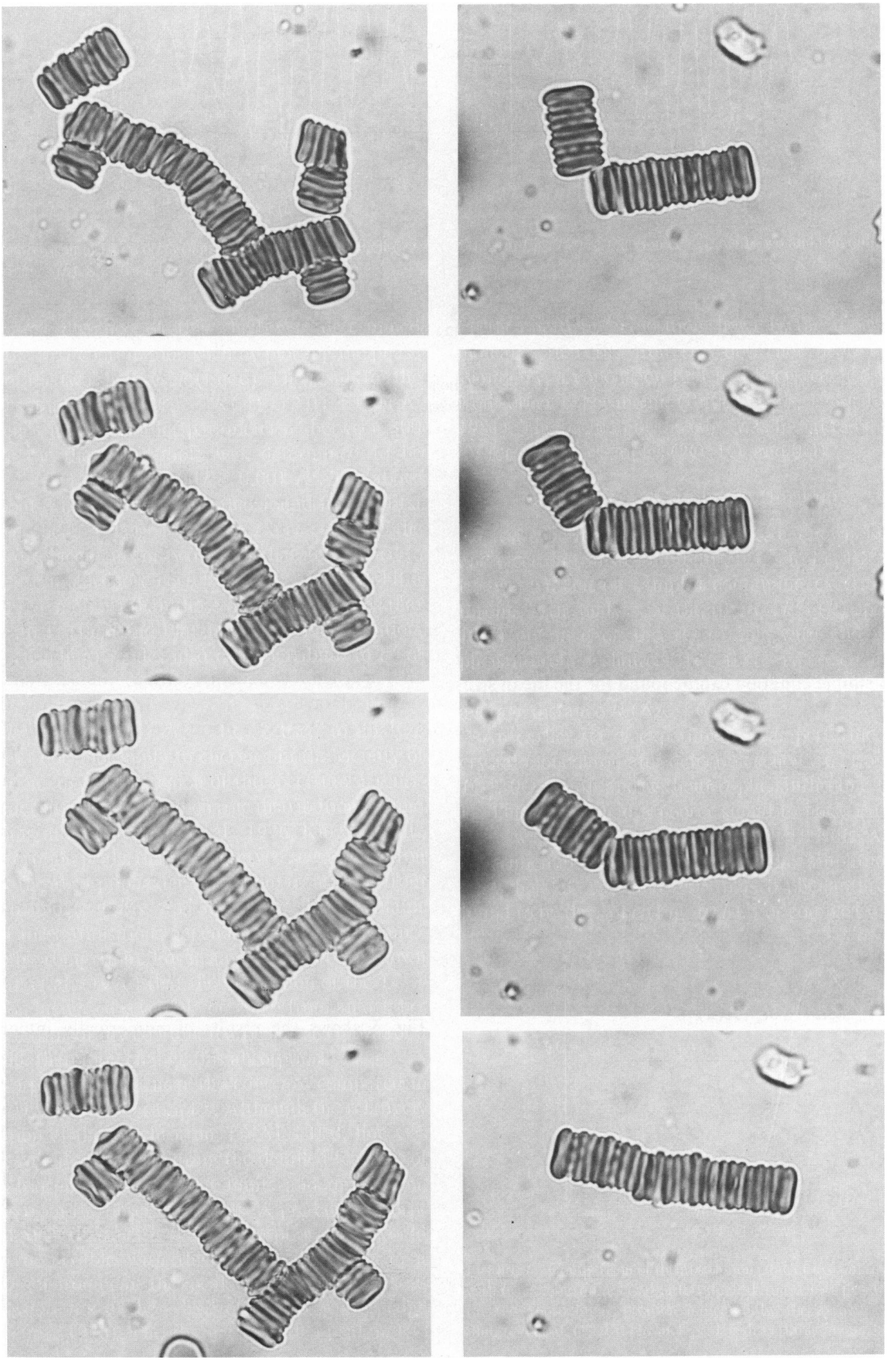

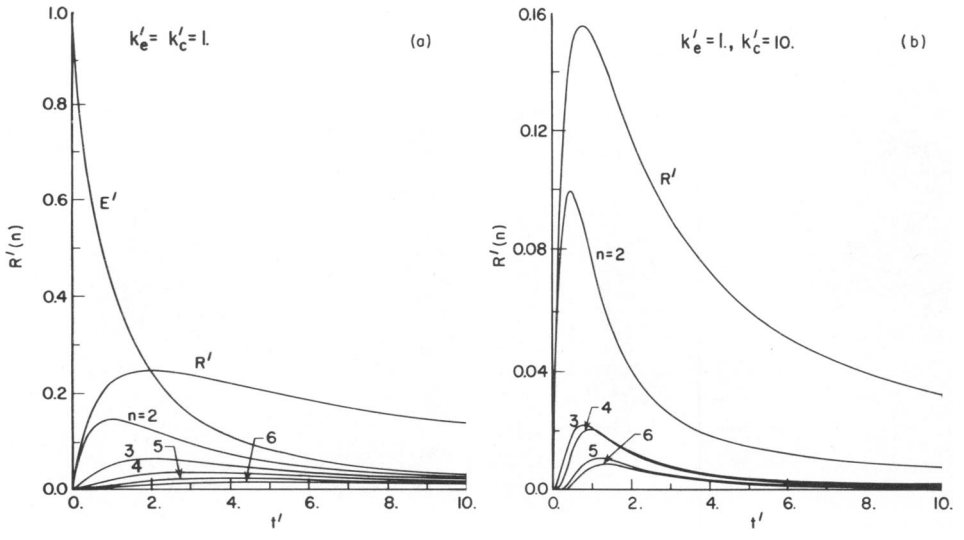

FIGURE 5 The kinetics of rouleau formation with a combined addition—condensation mechanism. E' is the free erythrocyte concentration, R' is the total concentration of rouleaux and $R'(n)$, $n = 2, 3, \ldots$ is the concentration of rouleaux with n cells. All variables including the time t' are nondimensional. (a) $k'_e = k'_c = 1.$, (b) $k'_e = 1.$ and $k'_c = 10.$

single aggregate, the equation for the concentration of rouleaux becomes

$$dR/dt = \tfrac{1}{2} k_e E^2 - \tfrac{1}{2} k_c R^2. \quad (12)$$

We have included a statistical factor of $\frac{1}{2}$ in each term since identical particles are reacting.

If we let $k \equiv k_e = k_a = k_c$, then as in the case of addition reactions a simple equation can be found for the mean size of a unit, U. From Eqs. 10–12 one finds

$$\frac{dU}{dt} = \frac{1}{2} kE_0, \quad U(0) = 1 \quad (13)$$

and hence

$$U(t) = 1 + \tfrac{1}{2} kE_0 t. \quad (14)$$

In the presence of condensation reactions, the following set of equations can be written for the concentration of rouleaux of size n:

$$dR(2)/dt = \frac{1}{2} k_e E^2 - k_a E R(2) - k_c R(2) \sum_{m=2}^{\infty} R(m), \quad (15)$$

$$dR(n)/dt = k_a E[R(n-1) - R(n)] + \frac{1}{2} k_c \sum_{m=2}^{n-2} R(n-m)R(m) - k_c R(n) \sum_{m=2}^{\infty} R(m), \quad n = 3, 4 \ldots, \quad (16)$$

where by convention a summation is zero when the upper limit is less than the lower limit; i.e., when $n = 3$ above. The condensation terms in Eq. 16 are derived by observing that an n-mer is formed by the collision of an m-mer with an $(n - m)$-mer. Such collisions occur with a frequency proportional to $R(m)R(n - m)$. Summing $R(m)R(n-m)$ from $m = 2$ to $n - 2$ counts every reaction twice, save that where $m = n - m$. The rate constant for the formation of an n–mer from two identical $(n/2)$–mers is multiplied by a statistical factor of $\frac{1}{2}$, hence we correct for the double counting and incorporate this statistical factor by multiplying the first sum in Eq. 16 by $\frac{1}{2}$. The second summation accounts for the loss of n-cell rouleaux by reaction with any other rouleau. As we show below, this equation is a simple generalization of the Smoluchowski equation.

One can nondimensionalize and simplify these equations by using Eq. 9 and Eq. 1, together with the additional definition

$$k'_c = k_c/k_a. \quad (17)$$

Fig. 5 shows the results of numerically integrating the nondimensional form of Eqs. 11, 12, 15, and 16 with initial conditions corresponding to a monodisperse system of red cells. In Fig. 5 *a* we examine the case in which $k'_e = k'_c = 1$. Comparing with Fig. 2 *b*, the results obtained when $k'_c = 1$ and $k'_c = 0$, one sees that the concentration of free erythrocytes decays slower when condensation of rouleaux occurs. This is easy to understand. When $k'_c > 0$ rouleaux coalesce and form fewer, but larger aggregates. Eq. 11 implies that in the presence of fewer rouleaux, erythrocytes undergo collisions less frequently with rouleaux, and consequently E decays slower. One might argue that when

two rouleaux condense the resulting aggregate should have a larger collision cross-section and thus compensate for the decrease in the rouleaux concentration. Consequently, k_a should not be constant, but rather should increase with rouleau size. This generalization will be dealt with in the next section.

Continuing the comparison between Figs. 2 *b* and 5 *a*, one sees that the inclusion of condensation causes R' to decrease at long times, rather than to asymptote to a constant value as $E' \rightarrow 0$ (Fig. 2*b*). At infinitely long times, Eqs. 11 and 12 predict $E' = R' = 0$ since all erythrocytes will eventually form rouleaux and all rouleaux will eventually condense. Our model does not predict the final state of the system to be one huge rouleaux with concentration $R' = 1/VE_0$. where V is the volume of the system. This can be remedied by replacing the term $-\frac{1}{2} k_c R'^2$ in Eq. 12 with the term $-\frac{1}{2} k_c R'(R' - 1/VE_0)$ so that each rouleau collides with all other rouleaux, but not with itself. If the total concentration of rouleaux $R' \rightarrow 0$ as $t' \rightarrow \infty$, then the concentration of rouleaux of size n, $n = 2, 3, \ldots, R'(n)$ must also decrease to zero as $t \rightarrow \infty$. This behavior is also shown by Fig. 5 *a*.

The effects of changing the parameters k'_e and k_c may also be explored via numerical integration. If k'_c is chosen less than one, say $k'_c = 0.1$, then curves resembling Fig. 2 *b* and Fig. 5 *a* are obtained, with R′ decreasing slower than in Fig. 5 *a* at long times and E' decreasing somewhat faster than in Fig. 5 *a* but not as fast as in Fig. 2 *b*. This is not surprising since Fig. 2 *b* is the result obtained when $k'_c = 0$. If k'_c is chosen much greater than one, say $k'_c = 10$, then a qualitatively different picture is obtained with $R'(n)$, $n = 2, 3, \ldots$, obtaining substantial peaks before decaying, as shown in Fig. 5 *b*.

Another way to study the effects of parameter changes is to examine the mean number of cells in a rouleau, $\langle n \rangle_r$ or the mean number of cells in a unit (a rouleau or a free erythrocyte), $\langle n \rangle_u$ defined as follows:

$$\langle n \rangle_r \equiv \frac{\sum_{n-2}^{\infty} nR'(n)}{\sum_{n-2}^{\infty} R'(n)} = \frac{1 - E'}{R'} \tag{18}$$

and

$$\langle n \rangle_u \equiv \frac{\sum_{n-1}^{\infty} nR'(n)}{\sum_{n-1}^{\infty} R'(n)} = \frac{1}{E' + R'} \tag{19}$$

where $R'(1)$ is defined to be E'. To be consistent with later notation for mean quantities we have called the mean number of cells in a unit $\langle n \rangle_u$ rather than U. The right sides of Eqs. 18 and 19 follow from the definition of R' (Eq. 1) and the conservation law for erythrocytes

$$E_0 = E + \sum_{n-2}^{\infty} nR(n). \tag{20}$$

In Fig. 6 we plot $\langle n \rangle_r$ and $\langle n \rangle_u$ vs. t' for $k'_e = 1$ and $k'_c = 0.1$, 1 and 10. When the rate of condensation, k'_c, is small compared to k'_e we again approximate the situation with addition reactions only. However, for pure addition systems $\langle n \rangle_r$ and $\langle n \rangle_u$ approach a constant limiting value as free erythrocytes are depleted. We see in Fig. 6 *a* that the rate of growth slows down as erythrocytes are depleted but does not go to zero, as condensation continues rouleau growth. When $k'_e = k'_c = 1$ (Fig. 6 *b*) both $\langle n \rangle_r$ and $\langle n \rangle_u$ increase linearly with time, as will be discussed more fully below. No distinction is made between addition and condensation with these parameters and the initial linear rise seen in Fig. 6 *a* simply continues. When $k'_e = 1$ and $k'_c = 10$ (Fig. 6 *c*), condensation is heavily favored and $\langle n \rangle_r$ increases rapidly. After erythrocytes are depleted the system behaves as if there were only a single rate constant, k_c, thus explaining why $\langle n \rangle_r$ and $\langle n \rangle_u$ increase linearly after an initial transient.

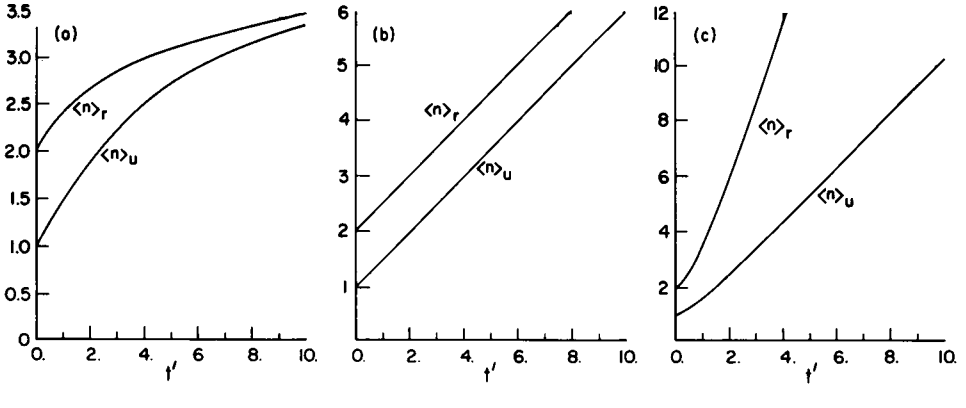

FIGURE 6 The kinetic behavior of the mean rouleau size $\langle n \rangle_r$ and the mean unit size $\langle n \rangle_u$ with a combined addition-condensation mechanism. (a) $k'_e = 1.$, $k'_c = 0.1$; (b) $k'_e = 1.$, $k'_c = 1.$; (c) $k'_e = 1.$, $k'_c = 10$.

The measured value of $\langle n \rangle_u$ for rouleau formation in normal human blood mediated by fibrinogen increases from 1 and saturates at ~8 as the concentration of fibrinogen is increased from 0.1 to 1.0 percent by weight (Jan and Chien, 1973*c*). From Fig. 6 one notes that including condensation in the aggregation model allows one to attain aggregates as large as the ones measured by Jan and Chien (1973*c*). To accurately verify a particular model with a particular set of parameter values more detailed experimental data would be required, such as the full rouleau number or weight distribution.

In Fig. 7 we show for $k'_e = k'_c = 1$ the computed rouleau number and rouleau weight distribution. Comparing these with Fig. 3 we see that with the inclusion of condensation, the concentrations of small roueaux rapidly decreases and the mass of the system is converted into large rouleaux. This is made particularly apparent by Fig. 7 *b* in which at $t' = 1$, 2, or 3 small aggregates predominate, and large aggregates (e.g., of size 14) are rare. However, by $t' = 20$ a large number of red cells are in aggregates of size 14 and larger, and the distribution curve is still increasing. Computing the mean size of a unit from Eq. 14, one finds $\langle n \rangle_u = 2.5$ at $t' = 3$. At $t' = 20$, $\langle n \rangle_u$ increases to 11 confirming the presence, at substantial concentrations, of aggregates larger than those illustrated in the figure.

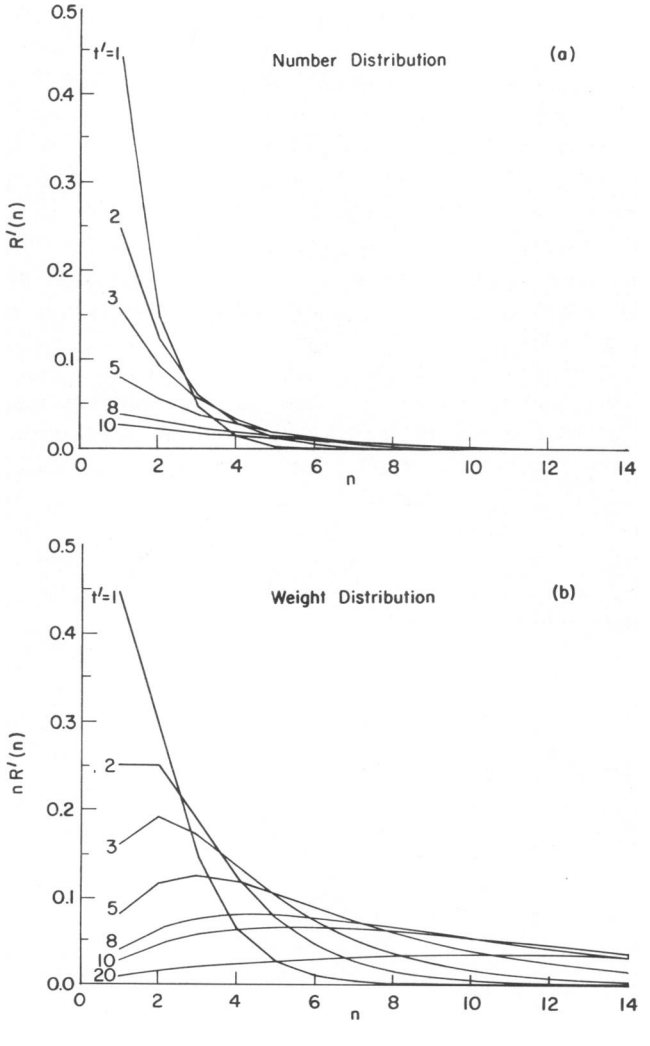

FIGURE 7 The distribution of rouleau for a combined addition-condensation mechanism. (*a*) The concentration of rouleaux in size n, $R'(n)$ vs. n. (*b*) The concentration of erythrocytes in rouleaux of size n, $nR'(n)$ versus n. Each curve is for a different value of t' as indicated and $k'_e = k'_c = 1$.

If we let R' (1) denote the nondimensional concentration of erythrocytes and use the values $k'_e = k'_c = 1$, one obtains the Smoluchowski equation

$$dR'(n)/dt' = \tfrac{1}{2} \sum_{m=1}^{n-1} R'(n-m)\, R'(m) - R'(n) \sum_{m=1}^{\infty} R'(m). \quad (21)$$

With the initial condition $R'(1, 0) = 1$, $R'(n, 0) = 0$, $n = 2, 3, \ldots$, it has the solution (cf. Perelson, 1980)

$$R'(n) = \left(\frac{t'}{2}\right)^{n-1} \Big/ \left[1 + \left(\frac{t'}{2}\right)\right]^{n+1}, \qquad n = 1, 2 \ldots, \quad (22)$$

shown in Fig. 5 *a*.

Using the Smoluchowski equation as the basis for a description of the kinetics of rouleau formation, Ponder (1927) found reasonable agreement with experimental data taken by turbulently shaking a dilute suspension of red cells in a test tube for short periods of time and then counting under a microscope the number of aggregates with one, two, three, ... cells. Only short times were examined and only aggregates of <12 cells were counted. To further test the merits of the Smoluchowski theory, Kernick et al. (1973) used the prediction that the mean unit size increases linearly with time according to $\langle n \rangle_u = 1 + t'/2$ (see Eq. 14). Using Eq. 22 one can also show that $\langle n \rangle_r = 2 + t'/2$. As $t' = kE_0t$, where $k = k_e = k_c = k_a$, a plot of the mean size of a unit or the mean size of a rouleaux against time should be a straight line with slope $\frac{1}{2} kE_0$. A plot of $\langle n \rangle_u$ or $\langle n \rangle_r$ at a fixed time vs. the initial erythrocyte concentration should also be linear.

Kernick et al. (1973) found that after an initial linear rise, curves of $\langle n \rangle_u$ vs. t flatten out and approach a steady state after about 30 min. Plotting the mean size of a unit at 10 min vs. hematocrit, Kernick et al. (1973) found that the data fit a straight line for hematocrits below 4%. At higher hematocrits they note that branch formation is observed so that the simple Smoluchowski model with a single rate constant is no longer applicable. Ponder used an hematocrit of ~2.5% in his experiments (Kernick et al, 1973), and did not report significant branch formation.

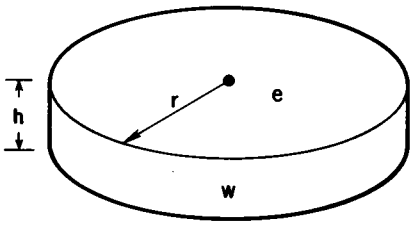

FIGURE 8 We model a red cell as cylindrical disk with radius r and thickness h. The disk has two ends with area e and a wall with area w.

III. DEGREE OF BRANCHING IN A ROULEAU

Model Geometry

The first step in describing the formation of branched chain rouleaux is the choice of a geometric description of the process and the selection of a set of variables to follow in the model. We treat the red cell as a flexible cylindrical disk of radius r and thickness h (Fig. 8). Its surface area can be thought of as divided into three parts: two faces or "ends" with area e, and one wall with area w. It should be clear that

$$e = \pi r^2 \tag{23}$$

and

$$w = 2\pi rh. \tag{24}$$

A branched rouleau is modeled as an aggregate of linear stacks connected at right angles. The red cells are thought to be sufficiently flexible to adhere to curved surfaces. The situation where one finds a symmetric "Y-shaped" branch (Fig. 9) is not explicitly considered in the theory, but taken to be the geometrical equivalent of the perpendicular "T-shaped" branch (Fig. 9). Symmetric branches are considered in Perelson and Wiegel (1982).

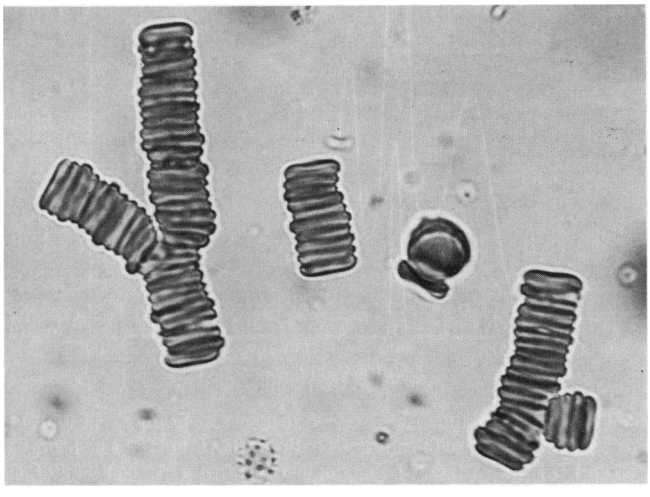

FIGURE 9 The geometry of rouleau branching. A symmetric "Y" branch and a perpendicular "T" branch.

Each linear, straight chain portion of a rouleau has two ends. The ends may either be free, or bound to the side of another stack. If the end is free, it is termed a cap, and if bound, it is termed a branch point. Each linear portion of a rouleau, however bound, is called a branch or segment. A particular rouleau might be described as having n cells, b branches, p branch points, and c caps. One can simply establish that if a rouleau has the topological form of a tree, i.e., has no cycles, then b, c, and p are all interdependent. The relationship between these variables can be found inductively, as follows: a cylindrical rouleau has two caps and one branch. Each addition of a branch also adds a cap. Hence, $c = b + 1$ for any rouleau. A particular rouleau may have many caps, though decidedly fewer caps than cells. A particular branch, by contrast, may have only zero, one, or two caps, as shown in Fig. 10. The non-cap ends of each segment are branch points (see Fig. 10). A rouleau with b branches has $2b$ branch ends; c of them are caps and the remaining p are branch points, so $2b = p + c$. For any rouleau, $c = b + 1$, so $p = b - 1$. Thus, choosing c as the independent variable,

$$b = c - 1 \text{ and } p = c - 2. \tag{25}$$

It should be noted that n and c do not form a complete description of any particular rouleau. Many rouleaux could be formed with n cells and c caps, where the distribution of cells along branches differs. Even specifying the number of cells and the number of caps belonging to every branch of a given rouleau would not provide a complete description, since many geometrical combinations of the branches are still possible. Thus we are abstracting only a small amount of the information needed to describe the system completely. Nevertheless, this description is sufficient to describe many of the functional characteristics of a rouleau and the kinetics of its growth. In their statistical mechanical treatment of the rouleau size distribution Wiegel and Perelson[1] show how to count the number of distinct rouleau with n cells and p branch points.

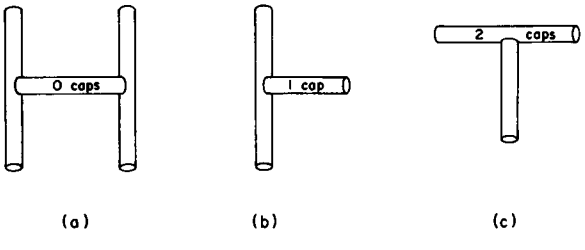

FIGURE 10 A rouleau segment may have 0, 1, or 2 free ends or caps. A bound end is a branch point. The labeled segment has 0 caps and 2 branch points in a, 1 cap and 1 branch point in b, and 2 caps and 0 branch points in c.

[1]Wiegel and Perelson. Manuscript submitted for publication.

The Probability of Branching

The tendency of rouleaux to form long unbranched chains is their most striking characteristic. With a simple model, we can examine the mechanism of the formation of these long rouleaux. Three assumptions are involved. First, rouleaux grow by single cells adhering to each other and to existing rouleaux. Second, collisions between single cells and rouleaux occur and result in cell adhesion with equal probability on any part of the external area of a particular rouleau. Third, in collisions sufficiently close to the end of a rouleau, the incoming cell will slide or "roll" to an equilibrium position at the end of the rouleau, while collisions far from the end of a rouleau will result in the initiation of a branch. The mechanism by which a cell moves to the end of a rouleau is not important in our model. The dynamics of such motions are discussed by Chien and Jan (1973) and Fung and Canham (1974).

The approach of the model is to postulate the existence of an "elongation zone" at each end of an unbranched rouleau. This zone includes the end surface with area e and the part of the wall within a critical distance r^* of the end of the rouleau (Fig. 11). The probability that a rouleau will branch when a red cell joins it is just the ratio of the area outside the elongation zone to the total area of the rouleau. Conversely, the probability that a rouleau will elongate when joined by a red cell is the area available for elongation divided by the total area.

The total surface area $A(n)$ of a straight chain rouleau composed of n cells is equal to the area of its two ends ($2e$) plus the area of its n external walls, or

$$A(n) = nw + 2e. \tag{26}$$

The area A^* upon which a collision will result in elongation is

$$A^* = 2(2\pi rr^* + e), \tag{27}$$

assuming $nh > 2r^*$. The probability $P_e(n)$ that the collision of a red cell with an n-cell rouleau will result in elongation of the rouleau is given by the ratio $A^*/A(n)$, i.e.,

$$P_e(n) = (2r^*/r + 1)/(1 + nh/r) \text{ for } n > 2r^*/h. \tag{28}$$

When the height of an existing stack of n red cells, nh, is

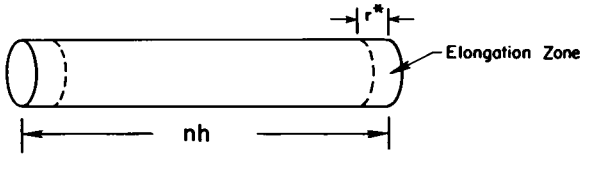

FIGURE 11 A straight chain rouleau with n cells and total length nh has two elongation zones each beginning a distance r^* from the end of the rouleau. We assume that a cell that lands with its center in an elongation zone will move to the end of the rouleau, whereas a cell that lands with its center outside of the elongation zone will initiate a branch.

$< 2r^*$ elongation must occur. Therefore

$$P_e(n) = 1 \text{ for } n < 2r^*/h. \tag{29}$$

Assuming cells add one at a time, $n - 1$ successive elongations are needed to form an n-cell rouleau without branches. The probability $P_s(n)$ that a randomly selected n-cell rouleau will be a straight chain is given by

$$P_s(n) = P_e(n - 1)P_s(n - 1)$$

or,

$$P_s(n) = \prod_{i=1}^{n-1} P_e(i), \quad n = 2, 3, \ldots, \tag{30}$$

where $P_s(1) = 1$ by definition.

Measurements of the geometry of human red cells establish that the typical erythrocyte has a volume of 94 μm^3 and a surface area of 135 μm^2 (Evans and Fung, 1972). Assuming that our cylindrical model of a red cell has these characteristics, then $h/r = 0.62$. A red cell is unlikely to climb to an equilibrium position at the terminus of a rouleau if its center lands appreciably more than a single red cell radius from the end of the rouleau. Thus r^* is probably $\leq r$, and it is useful to set $r^* = fr$, where $0 \leq f \leq 1$.

Fig. 12 *a* shows the values of P_e plotted vs. n for values of f between 0 and 1.0 and $h/r = 0.62$. The values of P_s are plotted vs. n for the same values of f and h/r in Fig. 12 *b*. As one might expect, Fig. 12 *a* shows that the elongation probability increases with the size of the elongation zone, i.e., with f. Notice that the ability of a cell to align itself on the end of a rouleau can have a striking effect on the elongation probability. From Eq. 28 we deduce that $P_e(n)$ increases threefold when $f = 1$ as compared to when $f = 0$. From Fig. 12 *b* we see that even with a maximal elongation zone, it is unlikely to find straight chain rouleaux with more than 13 or 14 cells. (Eq. 30 determines exactly how unlikely such events are). Thus large rouleaux are expected to be branched, and each branch, which would correspond to a straight chain rouleau in this theory, would generally be expected to contain at most 13 or 14 cells. Longer straight segments would appear but at a very low frequency. This upper limit of 13 or 14 depends on the ratio h/r and thus would vary somewhat among different species.

Notice this theory makes no predictions about how many n-cell rouleaux will form; it only gives information about the expected degree of branching in a population of n-cell rouleaux observed at any fixed time. Because we assume rouleaux grow by single cell addition, this theory is expected only to be valid for short times or for those experimental situations in which addition polymerization is a good kinetic model. The theory is not easily generalized to models involving other kinetic mechanisms, and it provides no information about the size distribution of branched rouleaux. To make further progress, we shall

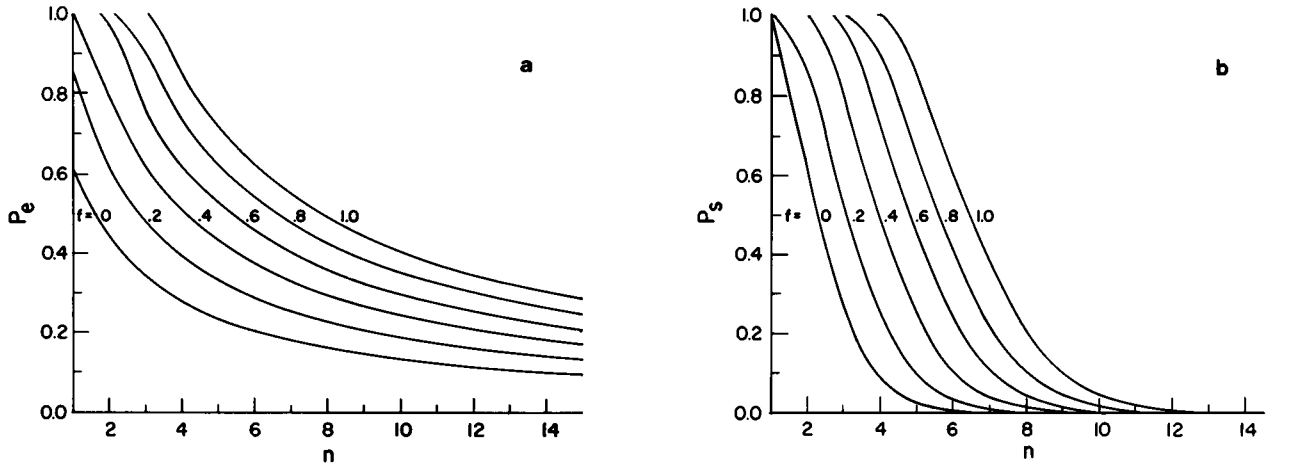

FIGURE 12 (*a*) The probability of a chain of length n being elongated $P_e(n)$ and (*b*) the probability of finding a straight chain of length n, $P_s(n)$, vs. the number of cells in the rouleau, n, for various values of $f = r^*/r$, assuming $h/r = 0.62$.

consider the detailed growth kinetics of branched rouleaux, following the techniques of polymerization kinetics.

Variables Describing Branched Rouleaux

For a detailed description of branched rouleaux, we introduce the variables E, $R(n, c)$, and $S(n, c)$, defined to be the concentrations of free erythrocytes, n-cell/c-cap rouleaux, and n-cell/c-cap straight chain segments in rouleaux, respectively. (Here, a straight chain or branch is taken to be a segment regardless of whether it is a free cylindrical rouleau or bound in a treelike rouleau).

The total concentration of branches or segments S and the total concentration of rouleaux R are defined as follows:

$$S = \sum_{n,c} S(n,c) \tag{31}$$

and

$$R = \sum_{n,c} R(n,c). \tag{32}$$

Let $\langle n \rangle_s$ and $\langle n \rangle_r$ denote the mean number of cells in a segment and in a rouleau, respectively, and let E_0 be the total concentration of erythrocytes in the system. By conservation of erythrocytes

$$E_0 = E + \langle n \rangle_r R, \tag{33}$$

and

$$E_0 = E + \langle n \rangle_s S. \tag{34}$$

Three additional variables are useful: M, the total number of caps per unit volume; T, the total area per unit volume belonging to the external surfaces of red cell aggregates; and W, the total area per unit volume belonging to the walls of the red cell aggregates. Free erythrocytes are excluded from designation as rouleaux or as segments, and likewise do not count as caps in M or contribute area to T and W. The concentration of caps M can be computed from

$$M = \sum_{n,c} cR(n, c). \tag{35}$$

Obviously, it is equally valid to write

$$M = \sum_{n,c} cS(n, c). \tag{36}$$

Likewise, if $A(n, c)$ is the external area of a rouleau with n cells and c caps, then T can be computed from

$$T = \sum_{n,c} A(n, c)R(n, c). \tag{37}$$

Lastly, if a_c is the external surface area of a single cap, then

$$W = T - Ma_c. \tag{38}$$

The simplest interpretation for a_c is the area of a face or end of a single red cell, e, as defined by Eq. 23. However, due to the presence of elongation zones at the ends of straight segments, there will be circumstances when we wish to consider $a_c > e$.

Only three of the six variables M, E, T, R, W, and S are independent. One connection is through the definition of W (Eq. 38). Another is a topological relationship between M, S, and R (see Eq. 43). The third relates T and E and R, and may be found by deriving an explicit formula for $A(n, c)$ as shown below. A rouleau is an aggregate of straight segments, and thus can be thought of as being formed by a process in which a single, long, straight chain rouleau is split successively, and the halves reattached differently (Fig. 13). The process shown can be carried out repeatedly to form a rouleau of any desired complexity.

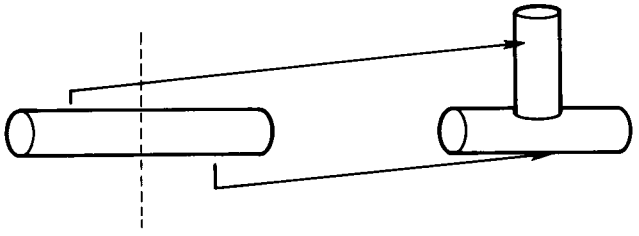

FIGURE 13 A branched rouleau can be formed by iteratively splitting a straight chain segment and reattaching the two halves as shown.

(Note that this is not a proposal for the mechanism of rouleau formation, but a construct to simplify thinking about the geometry.) What is notable about this process is that it conserves surface area. Breaking a rouleau in two creates two new faces each with area e. Attaching one of these faces on the side of a rouleau annihilates the same area $2e$, a face with area e is lost, as well as the area it adheres to on the side of the rouleau ($\sim e$). Consequently, to the order of our approximation, $A(n, c)$ is independent of c, so we need only find $A(n)$ for a straight chain rouleau. This is clearly given by

$$A(n) = nw + 2e. \tag{39}$$

Substituting this in Eq. 37, we find

$$T = (w\langle n\rangle_r + 2e)R. \tag{40}$$

The total area belonging to aggregates can also be found by a slightly different stratagem. Each bound cell contributes an area w, and each cap contributes an area e to the aggregate, but each branch point subtracts an area e from that contributed by the walls of the bound cells. A segment has 2 ends; c of them are free, so $(2 - c)$ of them are bound and form branch points. Hence

$$T = w(E_0 - E) + Me - e\sum_{n,c}(2 - c)S(n, c), \tag{41}$$

or, with the use of Eqs. 31 and 36,

$$T = w(E_0 - E) + 2Me - 2eS. \tag{42}$$

Combining Eqs. 33, 40, and 42 we find the surprisingly simple relation

$$M = S + R. \tag{43}$$

This conclusion can also be found inductively, and by the following alternate derivation: recall that

$$M = \sum_{n,c} cR(n, c)$$

and

$$c = b + 1.$$

Thus

$$M = \sum_{n,b} bR(n, b) + \sum_{n,c} R(n, c) = S + R, \tag{44}$$

where $R(n,b)$ is the concentration of rouleaux with n cells and b branches.

From a knowledge of E, R, and S, the mean values $\langle n\rangle_r$, and $\langle n\rangle_s$ can be found, as can the mean number of branches in a rouleau $\langle b\rangle$ (given by $\langle b\rangle = S/R$) and the mean number of caps in a rouleau $\langle c\rangle$ (given by $\langle c\rangle = M/R$). The necessary equations are given above.

Using the assumption that the process of rouleau formation occurs by a kinetic process whose rate is proportional to the area available for reaction, we can write equations for the time dependence of E, M, T, W, R, and S. The theory allows several different reactions to occur, each with an independent reaction rate per unit area. The details of the derivations are outlined next.

Kinetic Equations for Branched Rouleau Formation

The essence of our theory lies in delineating different types of reactions that may occur between erythrocytes and rouleaux or between different rouleaux, and in making the a priori assumption that for any particular reaction the reaction probability per unit area is equal everywhere on the external surface of all rouleaux. Consequently, we assume that the probability that a given rouleau will undergo any reaction in a unit time is proportional to its area available for that reaction. In each reaction, we shall assume that the rate of reaction is given by a rate constant per unit area k, times the available area for the reaction, times the concentration of cross-reactive species (either cells or caps).

To simplify thinking we view the collision of an erythrocyte with a rouleau as a point collision, the point of contact being the center of the incoming cell. Incorporating the notion of an elongation zone, we shall assume that if an erythrocyte strikes the face or possibility the wall of the last cell of a branch, then it will rapidly assume a position on the end of the branch, whereas a collision further from the cap will result in branching. Formalizing this notion we shall assign a "reactive area" a_c to each cap which denotes the total area upon which a collision with a red cell results in branch elongation. If the size of the elongation zone r^* is zero then $a_c = e$, i.e., only collisions on the end of a branch result in elongation. Alternatively, if a collision anywhere on the wall of the terminal cell of a branch results in elongation, then $r^* = h$ and $a_c = e + w$. For notational consistency we shall denote the reactive area of an erythrocyte a_e. When a red cell collides with another erythrocyte we shall assume that the collision can take place anywhere on the cell surface and still result in dimer formation with the cells adhering face to face. Thus the

total surface area of the red cell is reactive, i.e.,

$$a_e = 2e + w. \tag{45}$$

Although we are developing a kinetic theory of rouleau formation, we shall not explicitly deal with the kinetics of cell rolling and alignment on to the end of a growing rouleau. Rather, we simply assume that a cell which lands in an elongation zone moves to its position on the end of the branch at a rate which is sufficiently rapid compared to the cell collision rate that we can neglect the alignment time in our treatment of the overall kinetics.

In our condensation theory of rouleau formation we distinguish five types of reaction, each with a characteristic rate constant per unit area. First, two erythrocytes may collide to form a two-cell rouleau (Fig. 14 *a*). This is the prototype reaction whose mechanics have been worked out in the greatest detail (Skalak et al., 1977). Second, an erythrocyte may strike a cap and elongate the rouleau (Fig. 14 *b*). Third, an erythrocyte may strike the side of a rouleau and initiate a new branch (Fig. 14 *c*). Fourth, two caps may collide to form a longer branch (Fig. 14 *d*). Fifth, a cap may adhere to the wall of a rouleau (Fig. 14 *e*).

We neglect the possibility that the wall of one rouleau adheres to the wall of another rouleau at this stage in the development of our theory. Although lateral associations between rouleaux are seen, especially in systems with high adhesion energies (Fukada and Kaibara, 1980), such

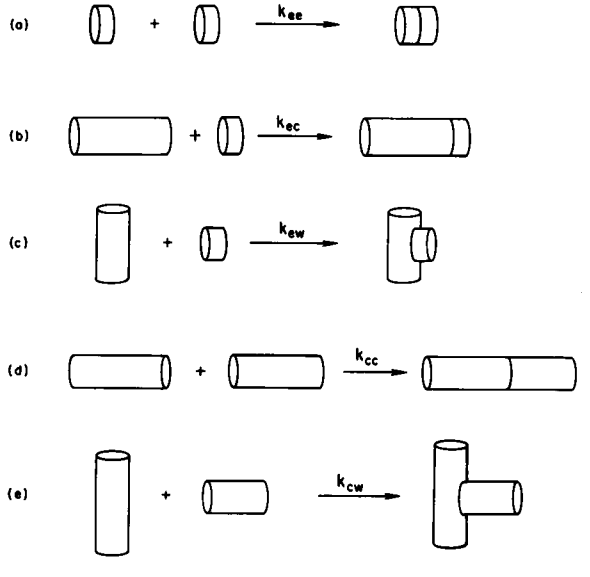

FIGURE 14 Diagrammatic representation of reactions that generate rouleaux. (*a*) Two erythrocytes react with rate constant per unit area k_{ee}, (*b*) An erythrocyte reacts with the cap on a rouleau with rate constant per unit area k_{ec}. This reaction elongates the rouleau. (*c*) An erythrocyte reacts with the wall of a rouleau to initiate a branch with rate constant k_{ew}, (*d*) Two rouleaux react via a cap-cap interaction with rate constant per unit area k_{cc}, (*e*) Two rouleaux react via a cap-wall interaction with rate constant k_{cw}.

contacts could occur over quite variable interaction areas, thus complicating our theory. According to Volger et al. (1973) rouleaux attached side by side are seen under pathological conditions, while under normal conditions only end-to-side attachments are seen. Consequently, our theory may not be applicable to rouleau formation in certain pathological states.

The concentration of erythrocytes changes with time as the result of the first three processes illustrated in Fig. 14. Therefore the differential equation for E has three terms; two erythrocytes are lost for each occurrence of the first reaction $[2E \rightarrow R(2, 2)]$, and one erythrocyte is lost per occurrence of the elongation reaction $[E + R(n, c) \rightarrow R(n + 1, c)]$ and per occurrence of the branch initiation reaction $[E + R(n, c) \rightarrow R(n + 1, c + 1)]$. Let k_{ee}, k_{ec}, and k_{ew} denote the rate constants per unit area of the erythrocyte-erythrocyte, erythrocyte-cap, and erythrocyte-wall reactions, respectively. Including a statistical factor of ½ for the erythrocyte-erythrocyte interaction one finds

$$dE/dt = -k_{ee}a_eE^2 - k_{ec}a_cME - k_{ew}EW. \tag{46}$$

where a_e and a_c are the reactive surface areas of an erythrocyte and a cap, respectively.

By similar reasoning, we find equations for the other variables mentioned. However, the remaining variables are affected by the condensation reactions as well as by addition reactions. We define two additional rate constants per unit area, k_{cc} and k_{cw}, to describe the cap-cap and cap-wall reactions, respectively. Caps are created by the erythrocyte-erythrocyte pairing (which generates two additional caps) and by the branch initiation reaction (which generates one). Similarly, caps are lost two at a time in the cap-cap condensation, and singly in the cap-wall reaction. Including statistical factors of ½ for the erythrocyte-erythrocyte and cap-cap reactions, we can write

$$dM/dt = k_{ee}a_eE^2 + k_{ew}EW - k_{cc}a_cM^2 - k_{cw}MW. \tag{47}$$

In a similar way, we can write an equation for the rate of change of the total external area, dT/dt. One difference, however, is that we now must consider the area added to rouleaux from each reaction, since T is an area concentration rather than a number concentration. The erythrocyte-erythrocyte reaction adds an area $2(e + w)$ for each occurrence and requires a statistical factor of ½. The elongation and branch initiation reactions each add a net external area w. The cap-cap reaction and the cap-wall reaction each absorb an area $2e$ per occurrence. Since the cap-cap reaction requires a statistical factor of ½, we find

$$dT/dt = a_e(e + w)k_{ee}E^2 + wk_{ec}a_cME + wk_{ew}EW - ek_{cc}a_cM^2 - 2ek_{cw}MW. \tag{48}$$

A differential equation for the reactive wall area per unit volume can be constructed from Eqs. 47 and 48 since $W \equiv T - Ma_c$. However, a direct derivation of the equation is more instructive. Recall that the reactive cap area a_c may be greater than e and therefore an area, $a_c - e$, must be subtracted from the wall area of each cell that forms a cap when computing W. As we explain below

$$dW/dt = [w - (a_c - e)]k_{ee}a_eE^2 + wk_{cc}a_cME + (w - a_c)k_{ew}EW + (a_c - e)k_{cc}a_cM^2 + (a_c - 2e)k_{cw}MW. \quad (49)$$

When two erythrocytes collide forming a two-cell rouleau, the reactive wall area is increased by $2w$, but then is decreased by $2(a_c - e)$ as two caps are also formed. Including a statistical factor of ½ gives the first term. In the second term, an erythrocyte adds to an existent cap and therefore extends a straight chain by one cell and adds an area w to W. When a red cell attaches to a wall the reactive wall area increases by w but decreases by two factors: $a_c - e$ due to the formation of a cap and by e due to the wall area covered by the red cell. Combining these factors gives the third term. In the cap-cap reaction, with statistical factor ½, two caps are lost and therefore an area $2(a_c - e)$ is gained as reactive wall area. Lastly, in a cap-wall reaction one cap is destroyed contributing a factor $a_c - e$ and an area e on the existent wall is covered by the newly attached cap.

Eqs. 46, 47, and 49 form a closed system so that numerical integration is immediately possible. From E, M, and W, one can find R and S. Using Eqs. 38, 42, and 43 we obtain

$$S = [(E_0 - E)w + (2e - a_c)M - W]/2e \quad (50)$$

and

$$R = M - S. \quad (51)$$

Alternatively, one can write differential equations directly for S and R. The joining of two erythrocytes creates new branches and new rouleaux. On the other hand, chain elongation due to the erythrocyte-cap reaction does not change S or R, and branch initiation due to the erythrocyte-wall reaction increases S but does not change R. Each occurrence of the cap-cap reaction results in the loss of a branch and of a rouleau, but the cap-wall reaction results only in the loss of a rouleau. Therefore

$$dR/dt = ½\, k_{ee}a_eE^2 - ½\, k_{cc}a_cM^2 - k_{cw}MW, \quad (52)$$

and

$$dS/dt = ½\, k_{ee}a_eE^2 + k_{ew}EW - ½\, k_{cc}a_cM^2. \quad (53)$$

Substitution of Eqs. 46, 47, and 49 into Eqs. 50 and 51 verified that the last two equations are entirely consistent with the previous five.

Proceeding in a similar way, one can write a coupled infinite set of differential equations for $R(n, c)$ and $S(n, c)$ that includes E, M, and W as variables. Since the equations are very complex, we treat them in Appendix II. The two systems $R(n, c)$ and $S(n, c)$ offer different information about the rouleau distribution, and neither can be used in any simple way to predict the other. The equations for $R(n, c)$ are infinite in number, as n and c are both theoretically unbounded, although $2 \leqq c \leqq n$. The system based on $S(n, c)$ is also infinite, but only in one dimension, as c only has values 0, 1, and 2. Therefore, the number of relevant equations is significantly smaller in the branch based system than in the rouleau based system.

In Appendix III, we derive from the detailed set of equations for $S(n, c)$, differential equations for the total concentration of segments with c caps,

$$S(c) \equiv \sum_{n=1}^{\infty} S(n, c), \quad c = 0, 1, 2.$$

These quantities are of interest for two reasons. First, they can be determined experimentally from photomicrographs of rouleaux. Second, once E, M, and W are known, a set of the three simple equations that can be solved numerically determine $S(0)$, $S(1)$, and $S(2)$. Thus predictions about the mechanism of rouleau formation can be tested without resort to examining the complete $R(n, c)$ or $S(n, c)$ distributions.

Numerical Solutions

Using numerical methods we can study the kinetics of branched rouleau formation. To reduce the number of parameters we nondimensionalize Eqs. 46–51 according to a scheme given in Appendix IV. With this nondimensionalization the rate constant describing the formation of a two-cell rouleau from free erythrocytes is taken as unity. If a free erythrocyte can react with a cap as easily as with another free erythrocyte, then $k_{ec} = k_{ee}$. Generally, with low concentrations of bridging macromolecules, a red cell cannot adhere as well to the side of a cylindrical rouleau as compared with its end, being unable to bring as much surface area into direct contact with the curved side of the rouleau. Thus k_{ew} and k_{cw} should be less than k_{ee}. At high concentrations of bridging macromolecules, or with longer macromolecules, branch formation may become more favorable. Thus the values of k_{ew} and k_{cw} will depend critically on the experimental conditions. For illustrative purposes we shall assume low adhesive energies, with k_{ew}, $k_{cw} \ll k_{ee}$. The cap-cap reaction involves the adherence of erythrocytes, generally face to face, but with potentially massive aggregates colliding. Thus $k_{cc} \leqq k_{ec}$. We will examine several possible values for k_{cc}.

We also need to specify the reactive cap area, a_c. This area is at least e, the area of a red cell face, but may be larger due to the presence of an elongation zone. In our simulations we shall assume $a_c = e + w$, i.e., an erythro-

cyte colliding with the wall of the terminal cell in a cylinder will move to the end of the cylinder and two caps that collide slightly off center will eventually align. With these assumptions and a_e given by Eq. 45, the only geometric data we require is h/r for a red cell. For a typical, unstressed, human red cell we shall choose $h/r = 0.62$ as before.

In Fig. 15 *a* we plot various means quantities vs. t' for $k_{cc} = k_{ee}$, $k_{cc} = 0.1\ k_{ee}$, and $k_{cw} = k_{ew} = 0.05\ k_{ee}$. Note $\langle n \rangle_u$ increases linearly and then slowly bends downward, reminiscent of the data reported by Kernick et al. (1973). For this range of times, the mean size of a rouleau remains small and there is not much branching, phenomena consistent with the observations of Kernick et al. Note that at $t' = 10$, $\langle n \rangle_r = 5.3$, $\langle n \rangle_s = 4.3$, and $\langle c \rangle = 2.2$. Fig. 15 *b* shows how E, R, and S vary with time. When free erythrocytes are consumed, rouleaux condense and their total concentration, R', decreases. Similarly, the concentration of straight segments, S', is reduced due to cap-cap interactions. If k_{cc} is increased to $0.5\ k_{ee}$, then more condensation occurs. As shown in Fig. 15 *c*, rouleau become longer (at $t' = 10$, $\langle n \rangle_r = 11.6$, $\langle n \rangle_s = 8.0$, $\langle c \rangle = 2.4$) and the concentrations R' and S' are reduced even further at long times (Fig. 15 *d*). The $\langle n \rangle_u$ curve also changes character, being concave up rather than concave down, reflecting the rapid decrease in both E' and R'. If k_{cc} is held constant at $0.5\ k_{ee}$ and the branching rate doubled so that $k_{cw} = k_{cw} = 0.1\ k_{ee}$ (not shown in Fig. 15), then at $t' = 10$, $\langle c \rangle$ increases to 3.1, segments become shorter, $\langle n \rangle_s = 7.3$, and the mean rouleau size increases to $\langle n \rangle_r = 15.9$. At this branching rate the mean rouleau would have two branches.

Rouleaux are more highly branched as k_{ew} or k_{cw} is increased further or if larger values of t' are examined. As shown in Fig. 15 *e*, $\langle c \rangle$ increases to 8.9 at $t' = 10$ if the branching rates are again doubled so $k_{ew} = k_{cw} = 0.2\ k_{ee}$. For these parameters, at $t' = 10$, the mean rouleau would have eight branch points, each straight segment would have mean length 6.3, and the whole rouleau would contain 50 cells. The very dramatic increase in the mean rouleau size as t' approaches 10 is due to rapid condensation of rouleau. At $t' = 10$ $R' = 0.02$ (Fig. 15 *f*) and is rapidly approaching zero.

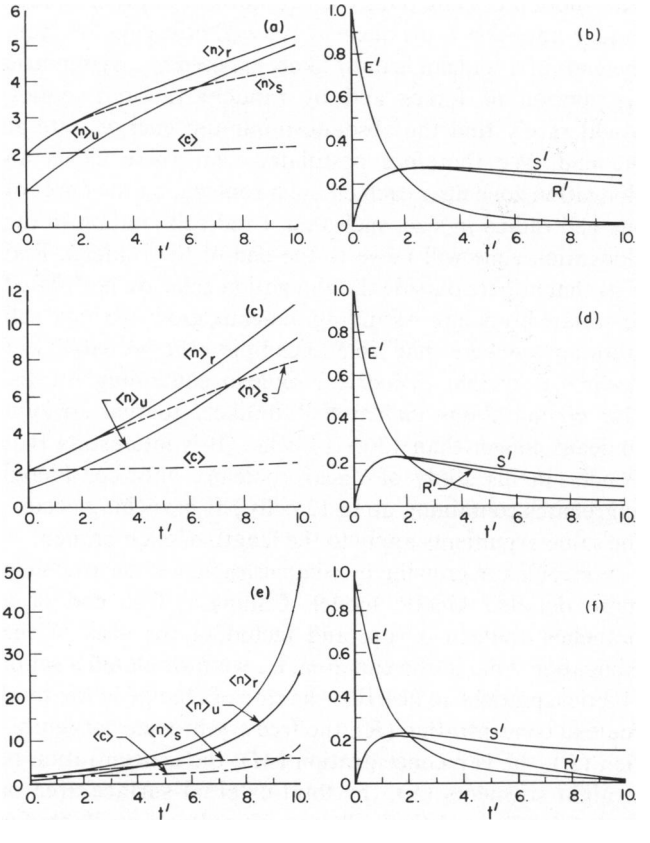

FIGURE 15 Dynamics of branched rouleau formation (*a*). A plot of $\langle n \rangle_u$, $\langle n \rangle_r$, $\langle n \rangle_s$ and $\langle c \rangle$ vs. time, for $k_{cc} = k_{ee}$, $k_{cc} = 0.1\ k_{ee}$, $k_{cw} = k_{ew} = 0.05\ k_{ee}$, $a_c = e + w$ and $h/r = 0.62$. With these parameter values $k'_{ee} = 0.692$, $k'_{cc} = 0.069$ and $k'_{cw} = k'_{ew} = 0.019$. (*b*) A plot of E', S' and R' vs. t' for the parameter values in (*a*). (*c*) Same as *a* except $k_{cc} = 0.5\ k_{ee}$. (*d*) E', R' and S' vs. t' for the parameter values in *c*. (*e*) Same as *a* except $k_{cc} = 0.5\ k_{ee}$ and $k_{ew} = k_{cw} = 0.2\ k_{ee}$. (*f*) A plot of E', S' and R' vs. t' for the parameter values in *e*.

IV. DISCUSSION

We have formulated a set of models to account for the kinetics of rouleau formation. Our approach based upon polymerization kinetics generalizes the work of Ponder (1927) who applied Smoluchowski's (1916, 1917) kinetic description of coagulation to rouleau formation. Like Ponder and Smoluchowski we have considered aggregation to stem from the formation of irreversible attachments between cells. Consequently, our models are limited to describing the early phases of rouleau formation during which dissociation kinetics can be ignored. In a later publication[2] we shall show how the ideas developed here can be extended to include disaggregation kinetics and phenomena such as loop formation which may become important in later stages of rouleau formation. Perelson and Wiegel (1982) have used statistical mechanical techniques to compute the equilibrium distribution of rouleau sizes. The kinetic studies that we are initiating here complement this work.

Our models are based upon the ideas of addition and condensation polymerization reactions. Assuming that a kinetic study of rouleau formation is begun with a monodisperse suspension of red cells, the predominant initial interactions should involve erythrocytes colliding to form pairs, the smallest aggregates which we consider to be rouleaux. As the reaction proceeds, red cells add to existent rouleaux, increasing their size, until all free erythrocytes are depleted. Using reasonable assumptions about rate constants, we showed that this addition process leads

[2]Samsel and Perelson. Manuscript in preparation.

to small rouleaux, in agreement with observations made using dextran as the bridging macromolecule.

As free erythrocytes become depleted, interactions between rouleaux must become the predominant reaction mechanism. Such condensation reactions can lead to very large rouleaux. If the interactions between free erythrocytes, between free erythrocytes and rouleaux, and between different rouleaux are all described by the same rate constant, then the Smoluchowski equation used by Ponder (1927) results. Even though this equation comprises an infinite system of quadratic nonlinear ordinary differential equations, it has a closed form solution that is easy to study. The equation predicts that the mean number of red cells per rouleau increases linearly with time. Thus, arbitrarily large rouleaux form, but owing to conservation of red cells, with vanishingly small concentrations. The experiments by Kernick et al. show that the linear growth of the mean unit size predicted by the Smoluchowski equation is only obeyed for short times (~20 min in their experiments). At longer times, the rate of growth of the mean unit size decreases and eventually the mean unit size approaches some final value. Kernick et al. (1973) also point out that the solution to the Smoluchowski equation predicts that the mean length a unit attains after a fixed reaction time rises linearly with the initial concentration of red cells, i.e., with E_0. Their experiments confirmed this behavior over the limited range of hematocrits studied, 0–4%.

In section II we generalized the Smoluchowski equation by using three separate rate parameters to describe erythrocyte-erythrocyte reactions (k_e), erythrocyte-rouleau reactions (k_a), and rouleau-rouleau condensations (k_c). When we assume these rate constants are not all equal, we have not been able to obtain a closed form solution to the resulting system of differential equations which determines the concentration of rouleaux of size n. However, numerical techniques can be applied to obtain solutions for reasonable sets of parameter values. By scaling the equations we need only specify two parameters: $k'_e = k_e/k_a$ and $k'_c = k_c/k_a$. If single erythrocytes react more frequently than aggregates, then $k'_e > k'_c$ and the mean rouleau size will initially rise linearly and then continue to increase, but with constantly decreasing slope as if it were approaching a saturation value (see Fig. 6 *a*). Thus one can qualitatively fit the kinetic data of Kernick et al. with this generalization of Ponder's model, although true saturation is only reached if $k'_c = 0$.

The behavior of $\langle n \rangle_u$ shown in Fig. 6 *a* depends upon $t' = k_a E_0 t$. Thus the same plot can be used to predict the behavior of $\langle n \rangle_u$ vs. E_0, for fixed t. The initial linear rise of this curve is consistent with the linear increase in mean unit size seen at low hemocrits by Kernick et al. (1973). However, if $k'_e > k'_c$ then we would predict that at hematocrits higher than those studied by Kernick et al. $\langle n \rangle_u$ would increase slower than linear as shown in Fig. 6 *a*.

Our generalization of Smoluchowski's equation still does not realistically represent all the dynamic features of rouleau growth. For example, the rate of addition of a single red cell to a rouleau is assumed to be constant, irrespective of the size of the rouleau. If a red cell can adhere to the wall of cylindrical rouleau, then one would expect the rate of such phenomena to depend upon rouleau size. Similarly, the rate of collision between rouleaux might be expected to depend on rouleau size. To incorporate these generalizations, we chose to model branch formation in rouleaux and make the rate constants of collision processes depend upon the area available for reaction. Long rouleaux having more surface area than small rouleaux will be more likely to have a branch initiated along their length.

Branching is generally rare among small rouleaux. Two red cells tend to adhere face to face, and if they adhere with other orientations they slide or roll relative to each other until this configuration is attained. A red cell adhering near the end of a rouleau can likewise move to the end and adhere face to face with the end cell. This motion is most likely due to an imbalance of forces on the red cell, with motion ceasing once the equilibrium position of face to face adhesion is attained. A red cell adhering far from the ends of a rouleau is most likely exposed to a symmetric distribution of forces and by random thermal motion would rarely find the absolute minimum energy state at the end. We therefore postulated that there exists an elongation zone near each end of a rouleau, on the order of one cell radius in size, such that a red cell landing in the elongation zone will move to the end of the rouleau. Red cells that adhere outside the elongation zone are postulated to initiate branches. Assuming rouleaux grow by single cell addition, we were than able to compute the probability of finding a straight cylindrical rouleau containing n cells. Our computations indicated it unlikely to find straight rouleaux longer than 13 or 14 cells. (It is interesting that Ponder in his study of linear rouleaux only considered aggregates containing up to 12 cells.) If branching occurs, the same arguments apply to the length of each branch.

For rouleaux growing by condensation, we constructed a more detailed kinetic model. Calling a free end of a branched rouleau a cap, and including the area of the elongation zone in the cap area, a_c, we formulated a set of kinetic equations to describe the rate of change in the total rouleau concentration (R), the free erythrocyte concentration (E), the cap concentration (M), the concentration of straight segments (S), the total external surface area of rouleaux (T), and the wall area of rouleaux available for branching (W). Using conservation equations, we showed that only three of these variables are independent. We also formulated two detailed sets of differential equations that determine the concentration of rouleaux containing n cells and c caps, $R(n, c)$, and the concentration of straight segments containing n cells and c caps, $S(n, c)$. Sufficiently detailed experimental determinations are not yet

available to confirm the predictions of this kinetic model. However, examining $\langle n \rangle_u$ we found that for reasonable parameter values $\langle n \rangle_u(t)$ increases linearly at early times as reported by Kernick et al. (1973), and then continues to increase but with decreasing slope. Also the values of $\langle n \rangle_u(t)$ are similar to those found by Kernick et al.

Adjusting the parameters in this model it is possible to obtain a large class of kinetic behaviors including the formation of only small unbranched rouleaux, the formation of large branched networks, and many intermediate structures. By analyzing the interactions among red cells in great detail it may be possible to predict the values of the various rate constants which describe rouleau elongation and branching and hence obtain a theory that predicts the characteristics of rouleaux formed under different experimental conditions. Although we have made no explicit assumptions about the mechanism of red cell and rouleau collision (e.g. Brownian motion, turbulent mixing), we have assumed that the rate constants per unit area are constant. Thus, more detailed calculations would be required for flow fields in which the collision rates depended upon the spatial position in the fluid.

Because we have taken the aggregation to be irreversible, our model becomes incorrect at long times. This stems from two related problems. First, irreversible aggregation is not a realistic model because in any physical situation breakup of rouleaux will eventually limit the size of aggregates. (Irreversible condensation implies that all of the cells will eventually end up bound together in a single large aggregate.) Second, as aggregates grow very large, the assumption that rouleaux will have a tree geometry (i.e., have no loops) becomes invalid because the probability that a cap will bind to another cap or wall on the same rouleau is no longer negligible. Thus, to describe the long-time behavior of rouleau formation requires that we consider both disaggregation and loop formation. In a later publication[2] we will show how to modify the present formulation to include these long-time effects and thus extend the validity of the model to situations in which equilibrium is attained.

APPENDIX I

Limiting Behavior of the Addition Model

Here we find the concentration of rouleaux and the mean unit size for a pure addition mechanism in the limit $t' \to \infty$ for $k_e' = 2$. This limit corresponds to the time at which all free erythrocytes have been incorporated into rouleaux.

With $k_e' = 2$, the nondimensional forms of Eqs. 2 and 4 reduce to

$$dR'/dt' = E'^2, \tag{A1.1}$$

and

$$dE'/dt' = -2E'^2 - E'R'. \tag{A1.2}$$

Letting

$$U = 1/(E' + R'), \tag{A1.3}$$

it is easy to see that

$$dU/dt' = UE', \tag{A1.4}$$

and

$$dE'/dt' = -E'^2 - E'/U. \tag{A1.5}$$

Dividing Eq. A1.5 by Eq. A1.4, we have

$$dE'/dU = -E'/U - 1/U^2.$$

Hence

$$d(UE')/dU = -1/U.$$

So

$$UE' = \ln U + 1, \tag{A1.6}$$

where 1 is the constant of integration needed to satisfy the conditions $E' = 1$ and $U = 1$ at $t' = 0$. Substituting Eq. A1.6 into Eq. A1.4 gives an equation that can be integrated to yield

$$t' = e[E_1(1 - \ln U) - E_1(1)], \tag{A1.7}$$

where $E_1(\cdot)$ is the exponential integral of order 1 (cf. Abramowitz and Stegun, 1970), $E_1(1) = 0.21938\ldots$, and e is the base of the natural logarithms. Unfortunately, the function $E_1(\cdot)$ has no explicit inverse and Eq. A1.7 can not be solved analytically for $U(t')$.

At large t, E' approaches 0, (intuitively, this may be used as an index of the extent of reaction for pure addition systems). Hence from Eqs. A1.6 and A1.3

$$\lim_{t' \to \infty} U(t') = e = 2.71828\ldots \tag{A1.8}$$

and

$$\lim_{t' \to \infty} R'(t') = 1/e = 0.367879\ldots. \tag{A1.9}$$

These limiting values are useful since they may be compared with experimental determinations.

APPENDIX II

Equations for $S(n, c)$ and $R(n, c)$

Incorporating the effects of branching in the study of the condensation kinetics of rouleau formation leads to much more complicated equations than were found for the theories neglecting branching. Fig. 14 shows the relevant reactions, and may be useful as a rough guide in formulating the equations in this appendix.

In writing a set of equations for $S(n, c)$ we need to pay special attention to $S(1, 1)$ and $S(2, 2)$. The erythrocyte-erythrocyte reaction creates two-cell, two-cap branches, and the erythrocyte-wall branch initiation process creates one-cell, one-cap branches. Both types of branches are lost through elongation. The cap-cap reaction, with rate $k_{cc}a_c MS(1, 1)$, and the cap-wall reaction with rate $k_{cw}WS(1, 1)$, each reduce the concentration of one-cell, one-cap branches. These branches are created only by the branch initiation process outlined above. Hence, we find

$$dS(1, 1)/dt = k_{ew}EW - k_{cc}a_c ES(1, 1) - k_{cc}a_c MS(1, 1) - k_{cw}WS(1, 1). \tag{A2.1}$$

By similar reasoning, we note that two-cell, two-cap branches are formed by the erythrocyte-erythrocyte reaction and lost by condensation. The condensation terms occur with twice the reactivity of those in the one-cap one-branch case, since condensation can occur on either cap of

S(2, 2). Hence,

$$dS(2,2)/dt = \tfrac{1}{2}k_{cc}a_cE^2 - 2k_{cc}a_cES(2,2) - 2k_{cc}a_cMS(2,2) - 2k_{cw}WS(2,2). \quad (A2.2)$$

It should be noted that $S(1, 2)$ represents branches that do not exist, and $S(2, 1)$ are described by the general equations that follow.

The general equations for $S(n, c)$ are best treated in three individual cases: $S(n, 0)$, $S(n, 1)$, and $S(n, 2)$. Each of these types of branches is formed through elongation, and/or through specific forms of cap-cap and cap-wall condensation. First, the concentration of doubly bound branches $S(n, 0)$ is unaffected by addition. The only way to form branches without caps is to condense a cap from an $S(n, 1)$ with a wall or with a cap from another $S(n, 1)$. Thus, one finds

$$dS(n,0)/dt = k_{cw}WS(n,1) + \tfrac{1}{2}k_{cc}a_c\sum_{k=1}^{n-1}S(k,1)S(n-k,1). \quad (A2.3)$$

The factor of $\frac{1}{2}$ in the summed expression is a correction for the duplication of terms in the sum as written.

Single-cap branches are created by the condensation of their caps with other caps or with walls. Hence,

$$dS(n,1)/dt = k_{cc}a_cE[S(n-1,1) - S(n,1)] + 2k_{cc}a_c\sum_{k=2}^{n-1}S(k,2)S(n-k,1) - k_{cc}a_cMS(n,1) + k_{cw}W[2S(n,2) - S(n,1)]. \quad (A2.4)$$

The factor of 2 in the summed term arises because $S(k, 2)$ has two caps and thus a double reactivity. The sum is asymmetric, so no double counting occurs.

In a similar manner one can write the equation for branches with two caps:

$$dS(n,2)/dt = 2k_{cc}a_cE[S(n-1,2) - S(n,2)] + 2k_{cc}a_c\sum_{k=2}^{n-2}S(k,2)S(n-k,2) - 2k_{cc}a_cMS(n,2) - 2k_{cw}WS(n,2). \quad (A2.5)$$

The summed term has a factor of 2 which is the product of two factors of 2 (double reactivity on each reactant) and one factor of $\frac{1}{2}$ (to correct for double counting in the sum).

Equations for $R(n, c)$ can also be written. Since $R(2, 2)$ is the only rouleau affected by the erythrocyte-erythrocyte reaction, we first construct the equation for $dR(2, 2)/dt$, and then find the general equation for $dR(n, c)/dt$. A two-cap, two-cell rouleau $R(2, 2)$ is formed by the joining of two erythrocytes and removed by the elongation reaction, by the cap-cap reaction or by cap-wall condensation. Hence we find:

$$dR(2,2)/dt = \tfrac{1}{2}k_{cc}a_cE^2 - 2k_{cc}a_cER(2,2) - 2k_{cc}a_cMR(2,2) - 2k_{cw}WR(2,2). \quad (A2.6)$$

All reactions in Fig. 14 except for the erythrocyte-erythrocyte reaction, contribute terms to the equations for $R(n, c)$. Thus,

$$\begin{aligned} dR(n,c)/dt &= ck_{cc}a_cE[R(n-1,c) - R(n,c)] \\ &+ k_{cw}E[(n-1)w + 2e - (c-1)a_c]R(n-1,c-1) \\ &- k_{cw}E[nw + 2e - ca_c]R(n,c) \\ &+ \frac{1}{2}k_{cc}\sum_{m=2}^{n-2}\sum_{d=2}^{c}[d(c-d+2)a_c]R(m,d)R(n-m,c-d+2) \\ &- k_{cc}a_cMc\,R(n,c) \\ &+ \frac{1}{2}k_{cw}\sum_{d=2}^{c-1}\sum_{m=2}^{n-2}A(m,n,c,d)R(m,d)R(n-m,c-d+1) \\ &- k_{cw}R(n,c)[M(nw + 2e - ca_c) + cW], \end{aligned}$$

$$n = 3, 4, \ldots, \quad 2 \le c \le n, \quad (A2.7)$$

where

$$A(m,n,c,d) = (c-d+1)[mw + 2e - da_c] + d[(n-m)w + 2e - (c-d+1)a_c]. \quad (A2.8)$$

Eqs. A2.7 and A2.8 can be understood, term by term, as resulting from the reactions already considered. The first three terms of Eq. A2.7 represent gain and loss of rouleaux by the elongation reaction, and by the erythrocyte-wall reaction. The reactive wall area in a rouleau with n cells and c caps is the total external area $A(n) = nw + 2e$ minus the total cap area, ca_c. The fourth term of the equation represents the growth of rouleaux due to cap-cap condensation, a reaction in which two caps are lost. The summand is the product of the area available for cap-cap condensation $[da_cR(m, d)]$, with the concentration of caps available for condensation $(c - d + 2)R(n - m, c - d + 2)$. Since the summation counts each term twice we divide by 2. The fifth term represents the loss of rouleaux by the same process. The sixth and seventh terms are the gain and loss (respectively) of rouleaux $R(n, c)$ due to cap-wall condensation, a reaction in which one cap is consumed. Since one rouleau with n cells and c caps is gained whenever $R(m, d)$ and $R(n - m, c - d + 1)$ condense via a cap-wall reaction, the appropriate reaction term contains their product times an area, $A(n, m, c, d)$. The area term contains two parts corresponding to the two ways in which the reaction may occur: the number of caps on $R(n - m, c - d + 1)$ multiplied by the wall area of $R(m, d)$ plus the number of caps on $R(m, d)$ multiplied by the wall area of $R(n - m, c - d + 1)$. The summation double counts the reaction terms leading to the inclusion of a factor of $\frac{1}{2}$. The seventh term of the equation also contains a similarly derived area factor.

The prototype equations for $R(n, c)$ and $S(n, c)$ contain areas that can become negative if no restriction is placed on the relationship between n and c. Obviously, we require the total area of any rouleau to be greater than its cap area; i.e.,

$$nw + 2e > ca_c. \quad (A2.9)$$

Thus the allowed values for c lie in the ranges

$$2 \le c \le n, \quad (A2.10)$$

and

$$c < (nw + 2e)/a_c. \quad (A2.11)$$

APPENDIX III

Distribution of Segments with Zero, One, or Two Caps

Without solving the full system of coupled equations for $S(n, c)$ or $R(n, c)$, we can predict the concentration of segments with c caps,

irrespective of n. Let us define

$$S(0) = \sum_{n=1}^{\infty} S(n, 0) \tag{A3.1}$$

$$S(1) = \sum_{n=1}^{\infty} S(n, 1), \tag{A3.2}$$

$$S(2) = \sum_{n=2}^{\infty} S(n, 2). \tag{A3.3}$$

These are related to the variables M and S by the equations

$$S = S(0) + S(1) + S(2), \tag{A3.4}$$

and

$$M = 2S(2) + S(1). \tag{A3.5}$$

Differential equations for these new variables can be found by summing Eqs. A2.1–A2.5 derived in Appendix II:

$$dS(0)/dt = \tfrac{1}{2}k_{cc}a_c S(1)^2 + k_{cw}WS(1), \tag{A3.6}$$

$$dS(1)/dt = k_{ew}EW + 2k_{cc}a_c S(1)S(2) - k_{cc}a_c MS(1) + k_{cw}W[2S(2) - S(1)], \tag{A3.7}$$

and

$$dS(2)/dt = \tfrac{1}{2}k_{ee}a_e E^2 + 2k_{cc}a_c S(2)^2 - 2k_{cc}a_c MS(2) - 2k_{cw}WS(2) \tag{A3.8}$$

APPENDIX IV

Nondimensional Form of the Equations for E, M, W, S, and R

Introducing the definitions

$$k'_{ec} = \frac{k_{ec}a_c}{k_{ee}a_e},\ k'_{ew} = \frac{k_{ew}w}{k_{ee}a_e},\ k'_{cc} = \frac{k_{cc}a_c}{k_{ee}a_e},\ k'_{cw} = \frac{k_{cw}w}{k_{ee}a_e},$$

$$E' = \frac{E}{E_0},\ M' = \frac{M}{E_0},\ W' = \frac{W}{wE_0},\ S' = \frac{S}{E_0},\ R' = \frac{R}{E_0},$$

$$t' = k_{ee}a_e E_0 t, \tag{A4.1}$$

Eqs. 46, 47 and 49–51 become

$$dE'/dt' = -E'^2 - k'_{ec}M'E' - k'_{ew}E'W', \tag{A4.2}$$

$$dM'/dt' = E'^2 + k'_{ew}E'W' - k'_{cc}M'^2 - k'_{cw}M'W', \tag{A4.3}$$

$$dW'/dt' = \frac{w - a_c + e}{w}E'^2 + k'_{cc}M'E' + \frac{w - a_c}{w}k'_{ew}E'W' + \frac{a_c - e}{w}k'_{cc}M'^2 + \frac{a_c - 2e}{w}k'_{cw}M'W', \tag{A4.4}$$

$$S' = \frac{1}{2e}[w(1 - E') + (2e - a_c)M' - wW'], \tag{A4.5}$$

$$R' = M' - S'. \tag{A4.6}$$

The various mean quantities that describe the distribution are given by

$$\langle n\rangle_r = \frac{1 - E'}{R'},\ \langle n\rangle_s = \frac{1 - E'}{S'},\ \langle n\rangle_u = \frac{1}{E' + R'}$$

$$\langle c\rangle = \frac{M'}{R'} \text{ and } \langle b\rangle = \frac{M'}{R'} - 1 = \frac{S'}{R'}, \tag{A4.7}$$

where $\langle n\rangle_r$, $\langle n\rangle_s$ and $\langle n\rangle_u$ are the mean lengths of a rouleau, a segment, and a unit (single cell or aggregate) respectively. The quantities $\langle c\rangle$ and $\langle b\rangle$ are the mean number of caps and branches per rouleau, respectively.

We would like to thank Dr. Richard Skalak for stimulating and encouraging discussions and Dr. George Bell for his helpful criticism. We also thank the Lambda Computer Center at Brown University and its director, Bill Shipp, for support. We dedicate this work to Aharon Katchalsky-Katzir, a pioneer of the macromolecular bridging hypothesis, whose spirit lives on despite his untimely death at the hands of terrorists. This work was performed in part under the auspices of the U.S. Department of Energy and was supported in part by BRSG grant S07 RR05664-11 awarded by the Biomedical Research Support Grant Program, Division of Research Resources, National Institutes of Health. A.S.P. is the recipient of an National Institutes of Health Research Career Development Award 7 K04 AI00450-02.

Received for publication 17 April 1981 and in revised form 18 August 1981.

REFERENCES

Abramowitz, M., and I. A. Stegun. 1970. Handbook of Mathematical Functions. Dover Publications, Inc., New York. 228–251.

Adler, P. M. 1979. A study of disaggregation effects in sedimentation. *AIChE (American Institute of Chemical Engineers) J.* 25:487–493.

Bell, G. I. 1981. Estimate of the sticking probability for cells in uniform shear flow with adhesion caused by specific bonds. *Cell Biophys.* 3:289–304.

Brooks, D. E., and G. V. F. Seaman. 1973. Some effects of dextran on human erythrocyte interactions. Proceedings of the 7th European Conference on Microcirculation, Aberdeen, 1972. Part I. *Bibl. Anat. No. 11.* Karger, Basel. 272–280.

Chang, H. N., and C. R. Robertson. 1976. Platelet aggregation by laminar shear and Brownian motion. *Ann. Biomed. Eng.* 4:151–183.

Chien, S., S. Usami, R. J. Dellenback, M. I. Gregersen, L. B. Nanninga, and N. M. Guest. 1967. Blood viscosity: influence of erythrocyte aggregation. *Science (Wash. D.C.).* 157:829–831.

Chien, S. 1973. Electrochemical and ultrastructural aspects of red cell aggregation. Proceedings of the 7th European Conference on Microcirculation, Aberdeen 1972. Part I. *Bibl. Anat. No. 11.* Karger, Basel. 244–250.

Chien, S., and K.-M. Jan. 1973. Ultrastructural basis of the mechanism of rouleaux formation. *Microvasc. Res.* 5:155–166.

Chien, S., S. Usami, K.-M. Jan., and R. Skalak. 1973. Macrorheological and microrheological correlation of blood flow in the macrocirculation and microcirculation. *In* Rheology of Biological Systems. H. L. Gabelnick and M. Litt, editors. Charles Thomas, Springfield, Ill. 12–48.

Chien, S., R. G. King, R. Skalak, S. Usami, and A. L. Copley. 1975. Viscoelastic properties of human blood and red cell suspensions. *Biorheology.* 12:341–346.

Chien, S. 1975. Biophysical behavior of red cells in suspensions. *In* The Red Blood Cell. D. Surgenor, editor. Academic Press, Inc., New York. 2:1031–1133.

Chien, S., L. A. Sung, S. Kim, A. M. Burke, and S. Usami. 1977. Determination of aggregation force in rouleaux by fluid mechanical technique. *Microvasc. Res.* 13:327–333.

Chien, S., A. L. P. Sung, M. L. Lee, J. Heldmen, K.-M. Jan, P. R. Zarda,

and R. Skalak. 1978. Role of membrane deformation in red cell rouleau formation. *J. Rheol.* 22:437.

Chien, S. 1980. Aggregation of red blood cells: an electrochemical and colloid chemical problem. *Adv. Chem. Ser.* 188:3–38.

Chien, S. 1981. Electrochemical interactions and energy balance in red cell aggregation. *In* Topics in Bioelectrochemistry and Bioenergetics. G. Milazzo, Editor. Wiley-Interscience Div., New York. 4:73–131.

Cokelet, G. R., E. W. Merrill, E. R. Gilliland, H. Shin, A. Britten, and R. E. Wells, Jr. 1963. The rheology of human blood-measurement near and at zero shear rate. *Trans. Soc. Rheol.* 7:303–317.

Dintenfass, L., and C. D. Forbes. 1973. About increase in aggregation of red cells with an increase of temperature in normal and abnormal blood. *Biorheology.* 10:383–391.

Dintenfass, L., and T. Somer. 1975. On the aggregation of red cells in Waldenstrom's macroglobulinemia and multiple myeloma. *Microvasc. Res.* 9:272–286.

Dintenfass, L. 1976. Rheology of Blood in Diagnostic and Preventive Medicine. Butterworth & Co., Ltd., London.

Dintenfass, L. 1977. Blood viscosity in severe diabetic and nondiabetic retinopathy. *Biorheology.* 14:151–157.

Evans, E., and Y.-C. Fung. 1972. Improved measurements of the erythrocyte geometry. *Microvasc. Res.* 4:335–347.

Fähraeus, R. 1921. The suspension-stability of the blood. *Acta Med. Scand.* 55:1–228.

Fukada, E., and M. Kaibara. 1980. Viscoelastic study of aggregation of red blood cells. *Biorheology.* 17:177–182.

Fung, Y. C. 1981. Biomechanics: Mechanical Properties of Living Tissues. Springer-Verlag, New York, Inc., New York. 62–91.

Fung, J. S. K., and P. B. Canham. 1974. The mode and kinetics of the human red cell doublet formation. *Biorheology.* 11:241–251.

Gauthier, F., H. L. Goldsmith, and S. G. Mason. 1971*a*. Particle motions in non-Newtonian media. *Rheol. Acta.* 10:344–364.

Gauthier, F., H. L. Goldsmith, and S. G. Mason. 1971*b*. Particle motions in non-Newtonian media II. Poiseuille flow. *Trans. Soc. Rheol.* 15:297–330.

Goldsmith, H. L., and S. G. Mason. 1967. The microrheology of dispersions. *In* Rheology: Theory and Applications. F. R. Eirich, editor. Academic Press, Inc., New York. 4:85–250.

Huang, C. R., N. Siskovic, R. W. Robertson, W. Fabisiak, E. H. Smitherberg, and A. L. Copley. 1975. Quantitative characterization of thixotrophy of whole human blood. *Biorheology.* 12:279–282.

Jan, K.-M. 1979*a*. Red cell interactions in macromolecular suspensions. *Biorheology.* 16:137–148.

Jan, K.-M. 1979*b*. Role of hydrogen bonding in red cell aggregation. *J. Cell Physiol.* 101:49–55.

Jan, K.-M., and S. Chien. 1973*a*. Role of surface electric charge in red blood cell interactions. *J. Gen. Physiol.* 61:638–654.

Jan, K.-M., and S. Chien. 1973*b*. Influence of the ionic composition of fluid medium on red cell aggregation. *J. Gen. Physiol.* 61:655–668.

Jan, K.-M., and S. Chien. 1973*c*. Role of the electrostatic repulsive force in red cell interactions. Proceedings of the 7th European Conference on Microcirculation, Aberdeen, 1972. Part I. *Bibl. Anat.* No. 11. Karger, Basel. 281–288.

Jones, M. N., and R. Perry, 1979. The kinetics of cellular aggregation induced by turbulent flow. *J. Theor. Biol.* 81:75–89.

Katchalsky, A., D. Danon, A. Nevo, and A. De Vries. 1959. Interactions of basic polyelectrolytes with the red cell. II. Agglutination of red cells by polymeric bases. *Biochim. Biophys. Acta.* 33:120–138.

Kernick, D., A. W. L. Jay, S. Rowlands, and L. Skibo. 1973. Experiments on rouleau formation. *Can. J. Physiol. Pharmacol.* 51:690–699.

Levich, V. G. 1962. Physicochemical Hydrodynamics. Prentice-Hall, Inc., Englewood Cliffs, N.J. 207–230.

Merrill, E. W., C. S. C. Cheng, and G. A. Pelletier. 1969. Yield stress of normal blood as a function of endogenous fibrinogen. *J. Appl. Physiol.* 26:1–3.

Perelson, A. S. 1980. Mathematical immunology. *In* Mathematical Models in Molecular and Cellular Biology. L. A. Segel, editor. Cambridge University Press, Cambridge. 365–439.

Perelson, A. S., and F. W. Wiegel. 1982. The equilibrium size distribution of rouleaux. *Biophys. J.* 37:515–522.

Ponder, E. 1927. On sedimentation and rouleau formation. II. *Quart. J. Exp. Physiol.* 16:173–194.

Purcell, E. M. 1978. The effect of fluid motions on the absorption of molecules by suspended particles. *J. Fluid Mech.* 84:551–559.

Reich, R. R. 1978. Hematology: Physiopathologic Basis for Clinical Practice. Little, Brown & Company, Boston.

Richardson, P. D. 1973. Effect of blood flow velocity on growth rate of platelet thrombi. *Nature* (Lond.). 245:103–104.

Ryan, V., T. R. Hart, and R. Schiller. 1980. Laser light scattering measurement of dextran-induced *Streptococcus mutans* aggregation. *Biophys. J.* 31:113–125.

Saffman, P. G., and J. S. Turner. 1956. On the collision of drops in turbulent clouds. *J. Fluid Mech.* 1:16–30.

Skalak, R., P. R. Zarda, K.-M. Jan, and S. Chien. 1977. Theory of rouleau formation. *In* Cardiovascular and Pulmonary Dynamics. M.-Y. Jaffrin, editor. Institut National de la Santé et de la Rechérche Medical. 71:299–308.

Smoluchowski, M. V. 1916. Drei Vorträge über Diffussion, Brownsche Molecularbewegung und Koagulation von Kolloidteilchen. *Physik. Z.* 17:585–599.

Smoluchowski, M. V. 1917. Versuch einer mathematischen Theorie der Koagulationkinetik Kolloider Lösungen. *Z. Phys. Chem.* 92:129–168.

Swift, D. L., and S. K. Friedlander. 1964. The coagulation of hydrosols by Brownian motion and laminar shear flow. *J. Colloid Sci.* 19:626–647.

Tanford, C. 1961. Physical Chemistry of Macromolecules. John Wiley & Sons, New York.

Thygesen, J. E. 1942. The mechanism of blood sedimentation. *Acta Med. Scand. Suppl.* 134:1–264.

Usami, S., R. G. King, S. Chien, R. Skalak, C. R. Huang, and A. L. Copley. 1975. Microcinephotographic studies on red cell aggregation in steady and oscillatory shear—a note. *Biorheology.* 12:323–325.

Volger, E., H. Schmid-Schönbein, and H. J. Klose. 1973. Rheological studies on the kinetics of artificial red cell aggregation induced by dextrans. Proceedings of the 7th European Conference on Microcirculation, Aberdeen, 1972. Part I. *Bibl. Anat.* No. 11. Karger, Basel. 83–90.

Whitmore, R. L. 1968. Rheology of the Circulation. Pergamon Press, Oxford. 1–196.

Ziff, R. 1980. Kinetics of polymerization. *J. Stat. Phys.* 23:241–263.